The energy spectrum using data of the Pierre Auger Observatory

Francesco Fenu
INAF – Osservatorio Astrofisico di Torino

Torino, 11/02/2021

Photo: Steven Saffi,
University of Adelaide

Introduction

- Introduction
- The Pierre Auger Observatory
- Main results of the Pierre Auger Observatory
- Overview of the Pierre Auger spectrum
- The SD1500 spectrum
- The interpretation of the spectral shape

Cosmic Ray energy spectrum

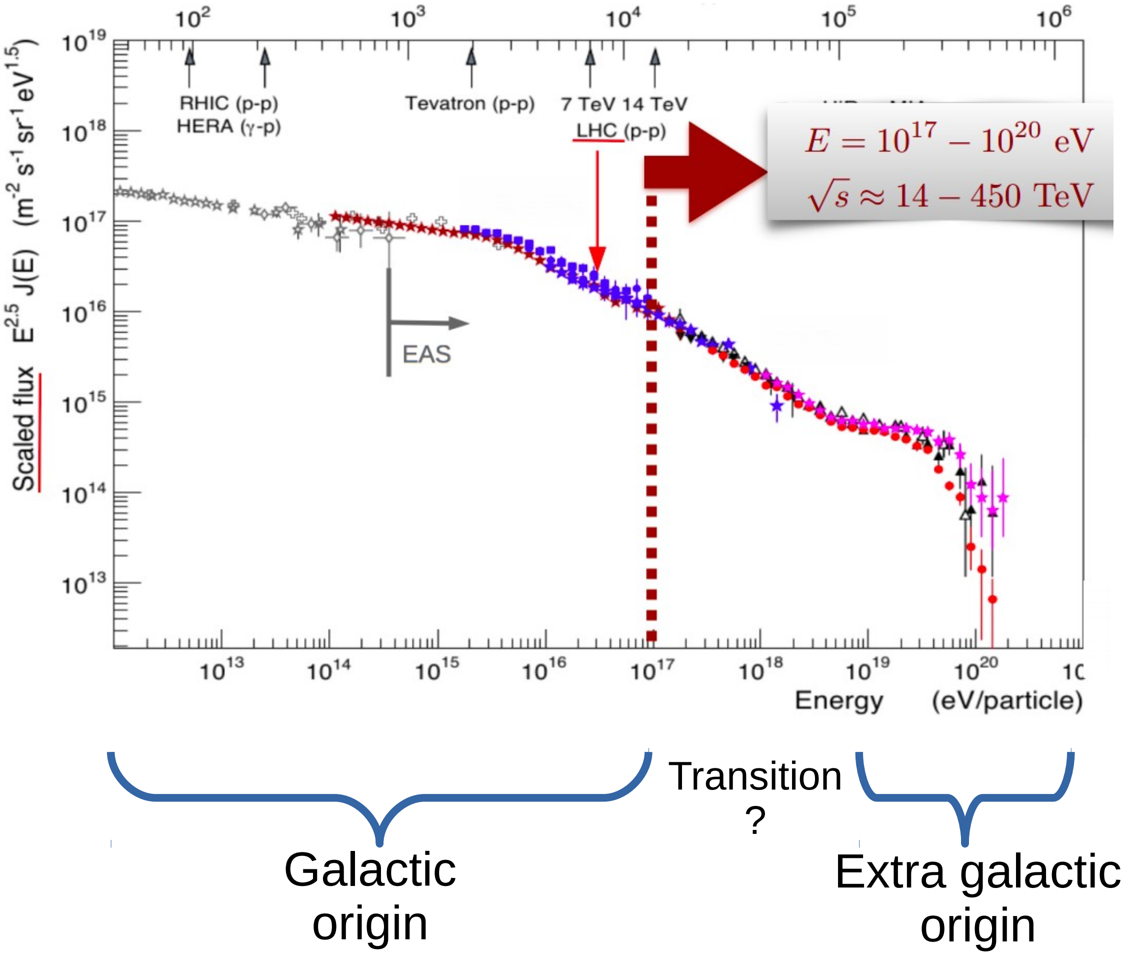

Sequence of power laws with several changes of steepness

- Knee (~10^{15} eV)
- Second Knee (~10^{17} eV)
- Ankle (~5×10^{19} eV)
- Steepening (~10^{19} eV)
- Suppression (~5×10^{19} eV)

Shape of spectrum fundamental to constrain astrophysical models

- Sources of UHECR?
- Nature of suppression
- Phenomenology of transition region
- Can we do UHECR astronomy?

Energy of UHECRs far above the one achievable by present accelerators

The Pierre Auger Observatory

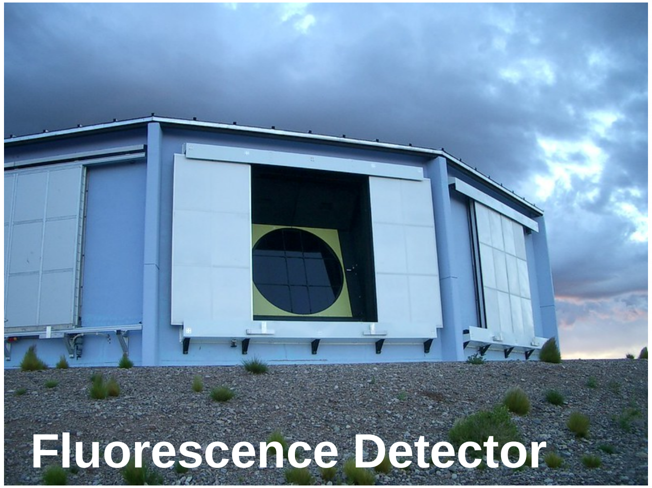

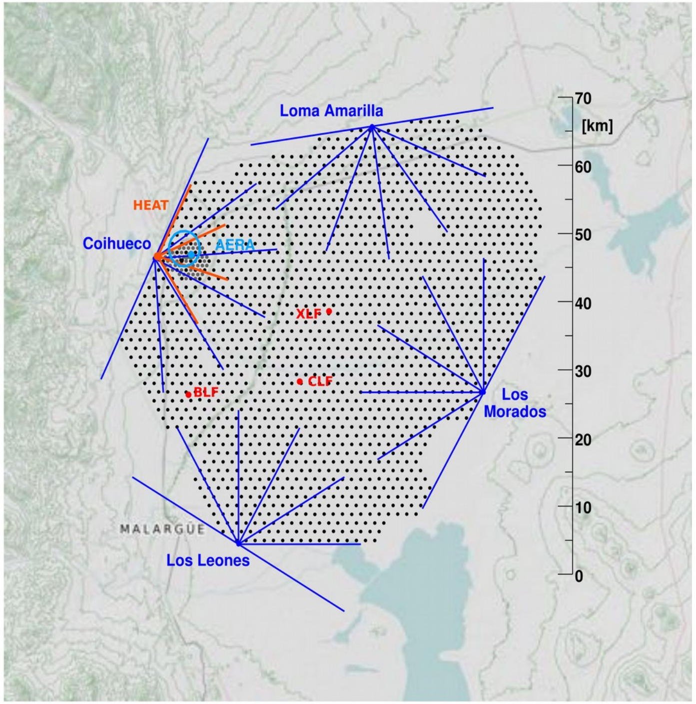

Surface detector (SD)

- **1500 m array**
  3000 km^2 – 1600 detectors
  1500 m grid
  E > 2.5 Eev

- **750 m array**
  24 km^2 – 61 detectors
  750 m grid
  E > 0.1 EeV

Fluorescence detector (FD)

- **24 telescopes in 4 building**
  Elevation 0-30^0
  E > 1 EeV

- **3 additional telescopes**
  Elevation 30-60^0
  E > 0.1 EeV

“The Pierre Auger Cosmic Ray Observatory”, NIM A 798 (2015) 172-213

The Fluorescence Detector

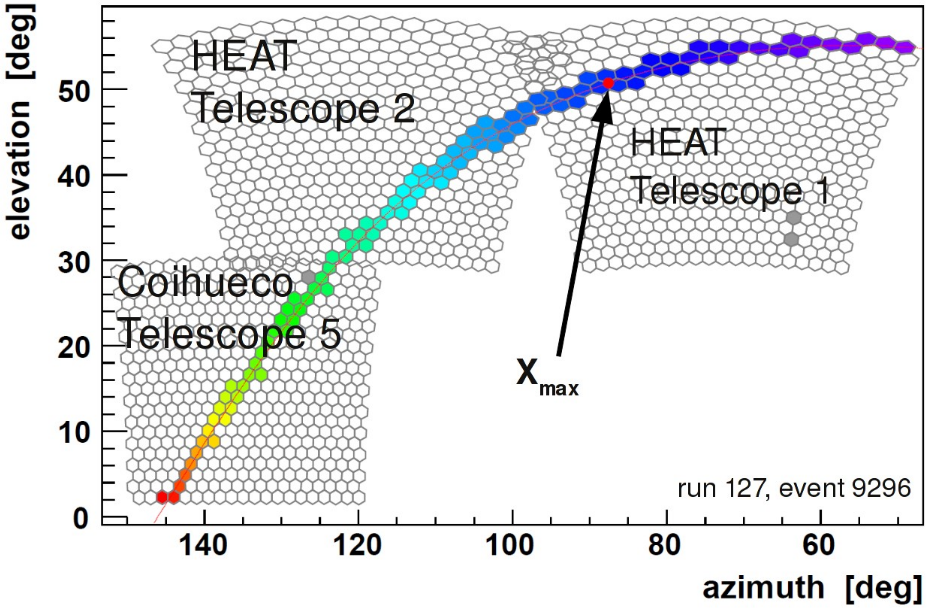

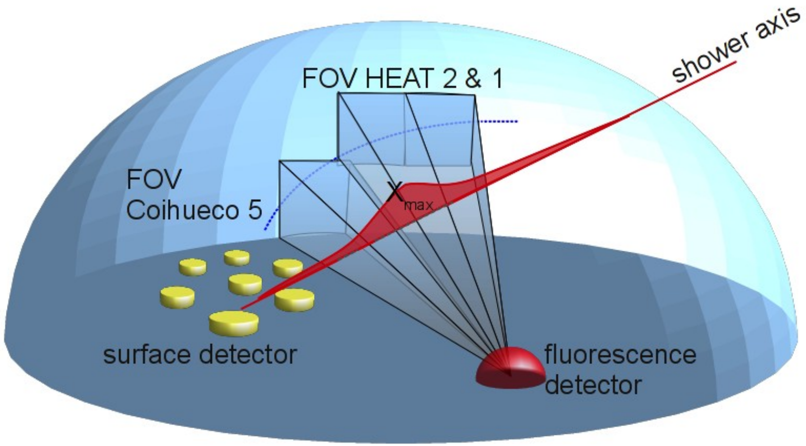

Detection of shower longitudinal profile through:

- Fluorescence
- Cherenkov

The Surface Detector

Detection of Cherenkov emission in water

Multi-level trigger to reject random muons

Reconstruct the geometry and shower size by means of ground detectors

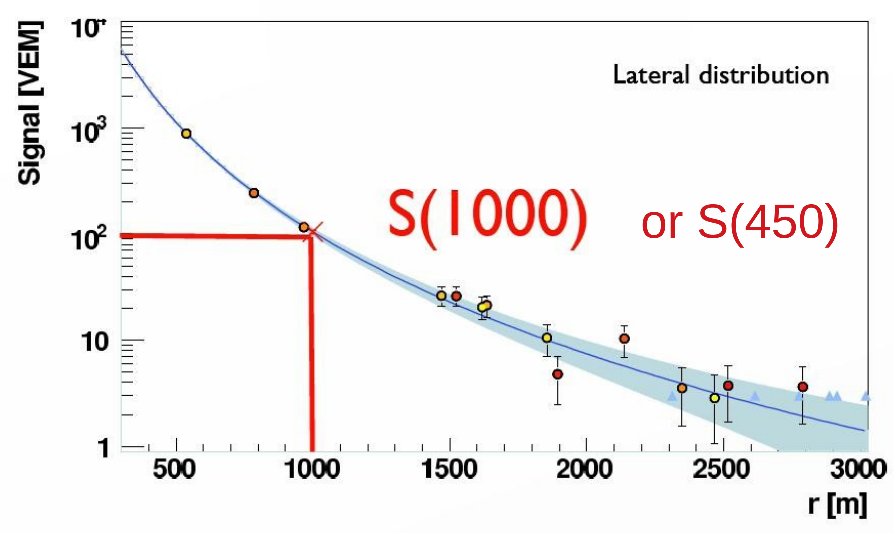

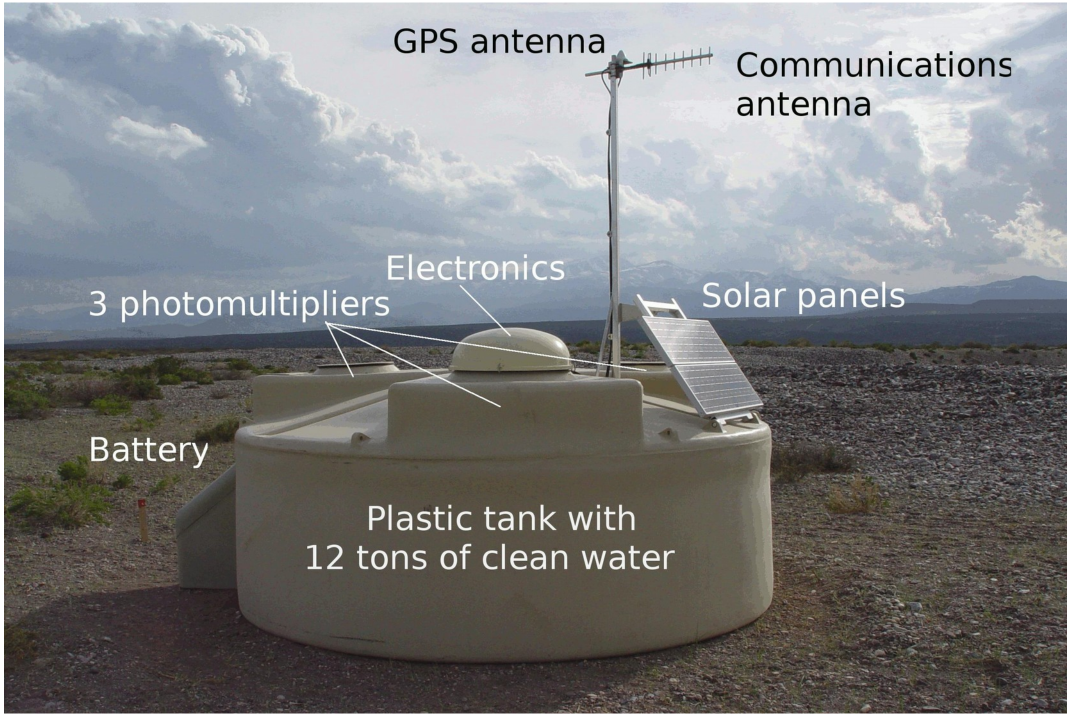

Three 9-inches photomultipliers to detect Cherenkov emission in water

The hybrid detection

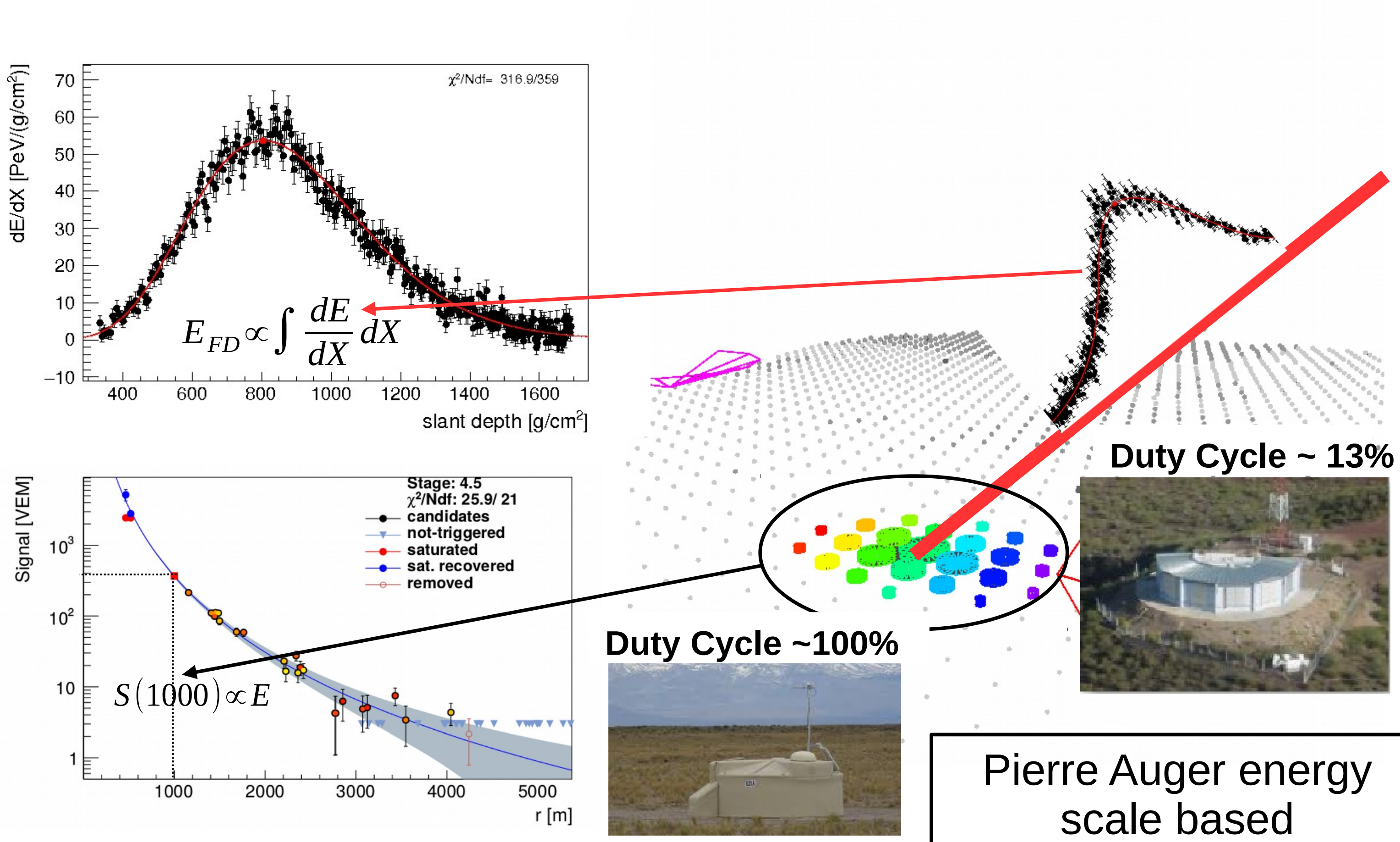

Energy scale
systematic uncertainty
14%

- FD calibration: 9.9%
- Fluor. Yield: 3.6%
- Atmosphere: 3.4-6.2%
- Energy deposit: 6.5-5.6%
- Stat. Uncert. Calib.: ~0.7-1.8%
- Invisible energy: ~3-1.5%
- Stability of the energy scale: 5%

Pierre Auger energy
scale based
on golden hybrid events

Main results: spectrum

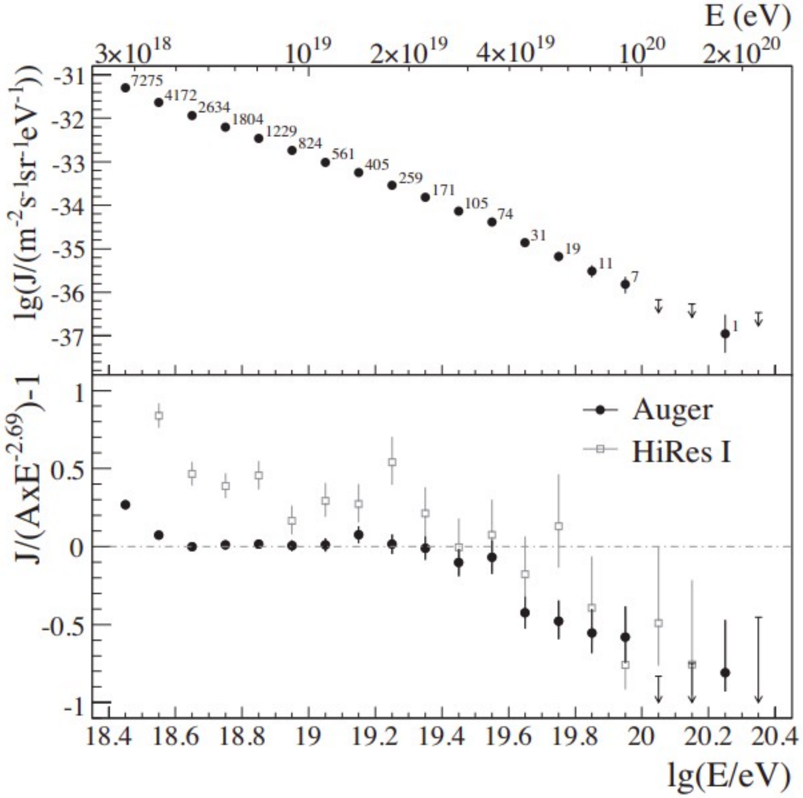

Suppression of the spectrum above ~4×10^{19} eV

Phys Rev. Lett. 101:061102 (2008)

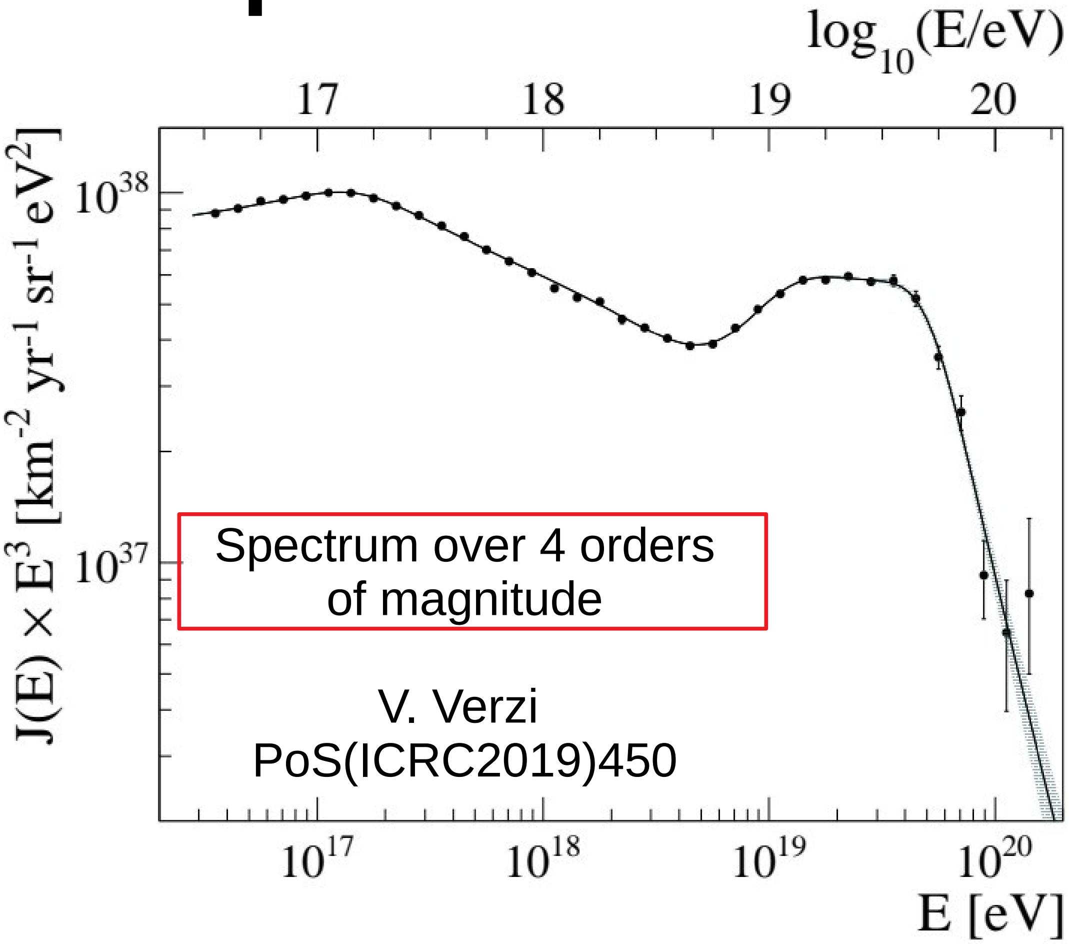

Spectrum over 4 orders of magnitude

V. Verzi
PoS(ICRC2019)450

Main results: large scale anisotropy

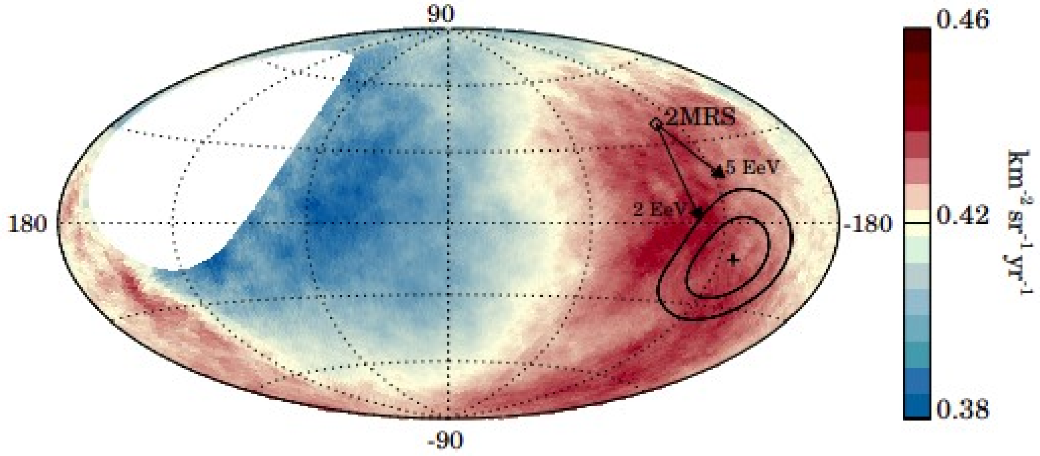

Measurement of a large scale anisotropy
Above 8×10^{18} eV
Science Vol. 357 1266 (2018)

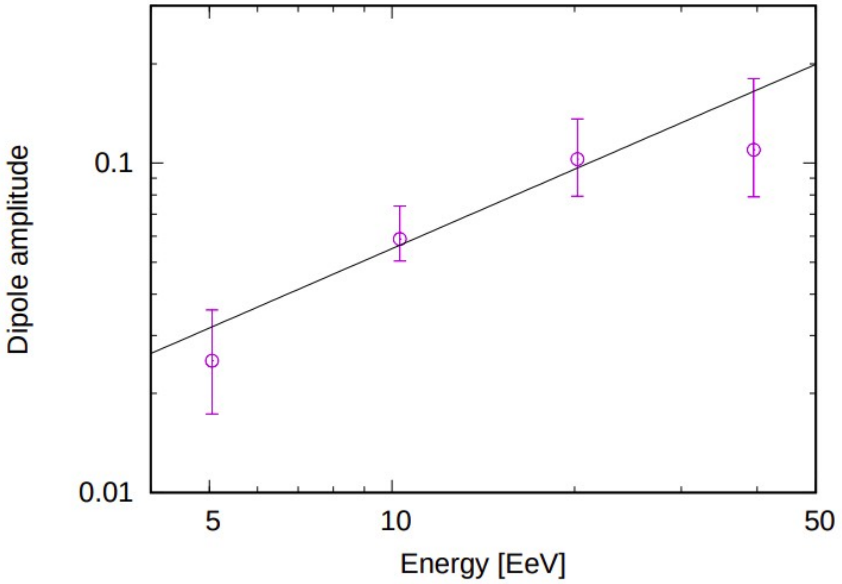

Dipole amplitude increases with energy
A. Aab et al. 2018, ApJ 868:4

Extragalactic origin of UHECR confirmed
(Dipole oriented 125 degrees away of GC)

Main results: large scale anisotropy

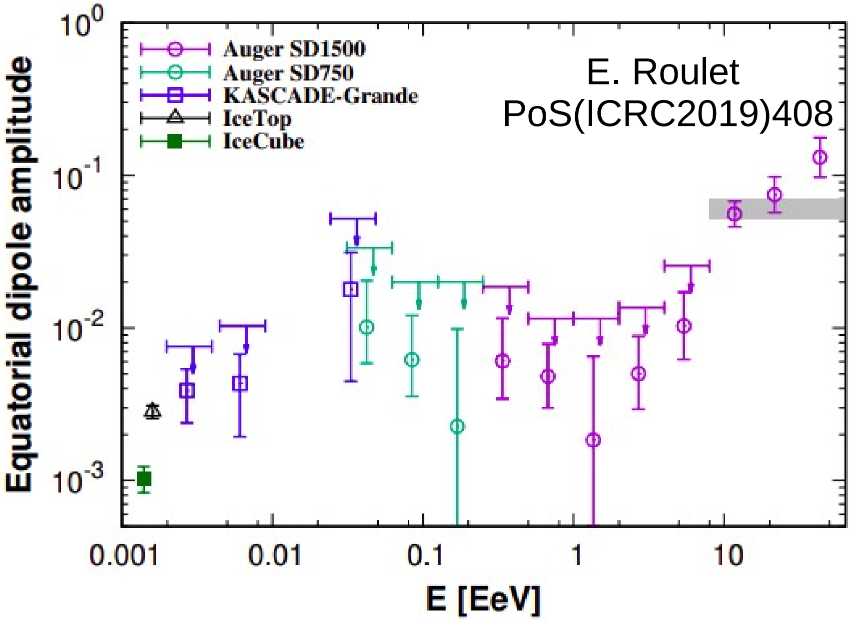

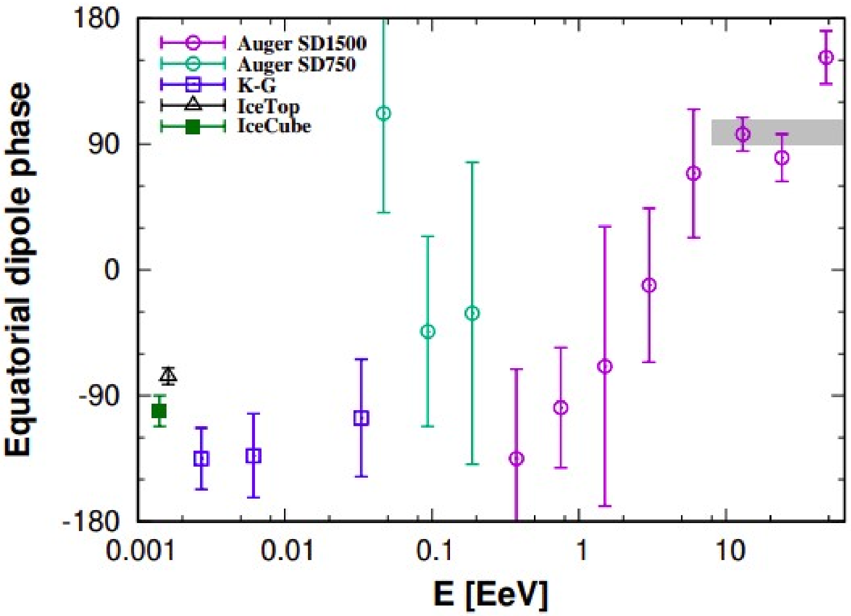

- The dipole is statistically significant only above 8×10^{18} eV
- Phase consistent with galactic center (up to ~10^{18} eV)
- Phase possibly aligned with nearby extragalactic matter above 8×10^{18} eV

Transition from galactic to extragalactic CR?

Main results: intermediate scale anisotropy

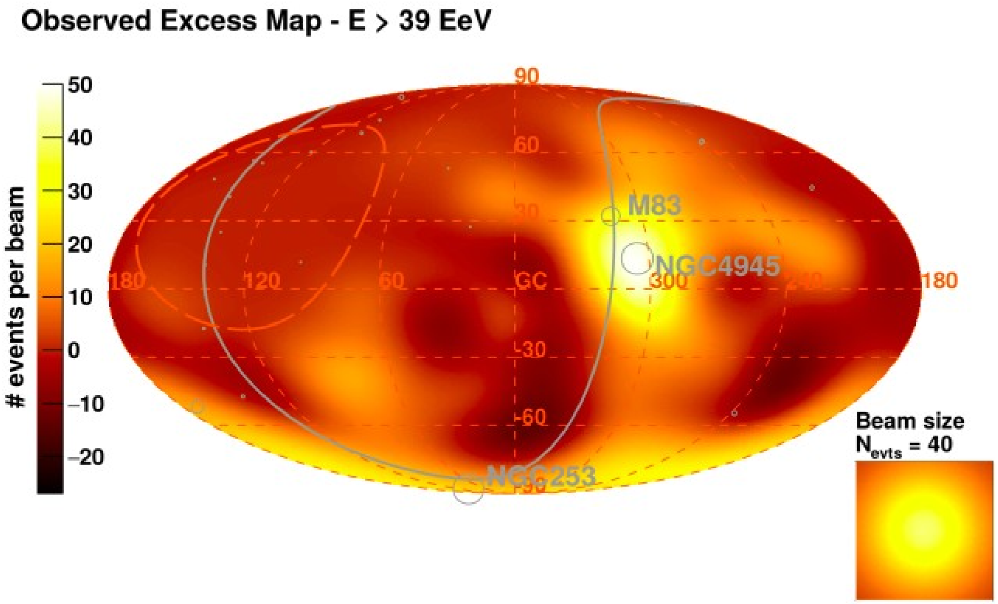

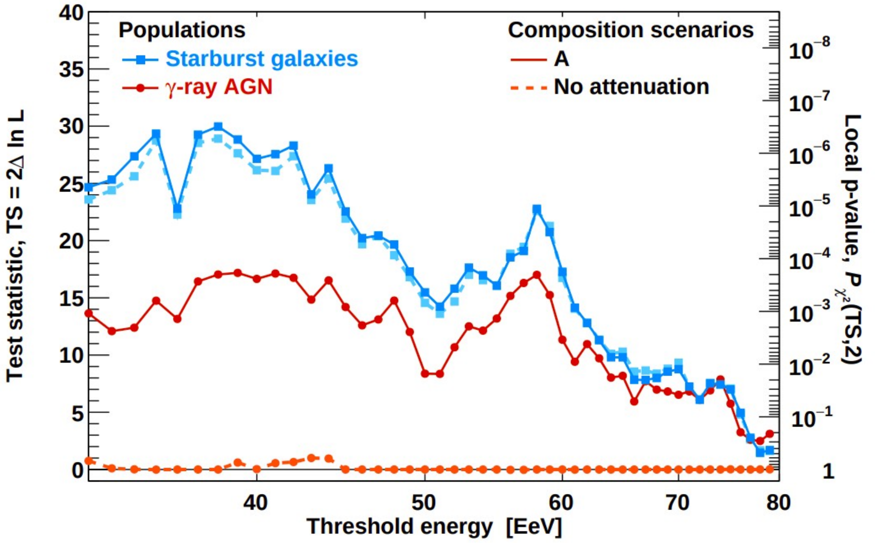

Catalog	E_{th}	TS	Local p-value	post-trial	f_{aniso}	θ
Starburst	38 EeV	29.5	4×10^{-7}	4.5 σ	$11^{+5}_{-4}\%$	$15^{+5}_{-4}{}^\circ$
γ–AGN	39 EeV	17.8	1×10^{-4}	3.1 σ	$6^{+4}_{-3}\%$	$14^{+6}_{-4}{}^\circ$
Swift-BAT	38 EeV	22.2	2×10^{-5}	3.7 σ	$8^{+4}_{-3}\%$	$15^{+6}_{-4}{}^\circ$
2MRS	40 EeV	22.0	2×10^{-5}	3.7 σ	$19^{+10}_{-7}\%$	$15^{+7}_{-4}{}^\circ$

Indication of anisotropy at small medium scale correlated with extragalactic sources

ApJ Lett. 253: L29 (2018)

L. Caccianiga
PoS(ICRC2019)206

Main results: intermediate scale anisotropy CEN-A

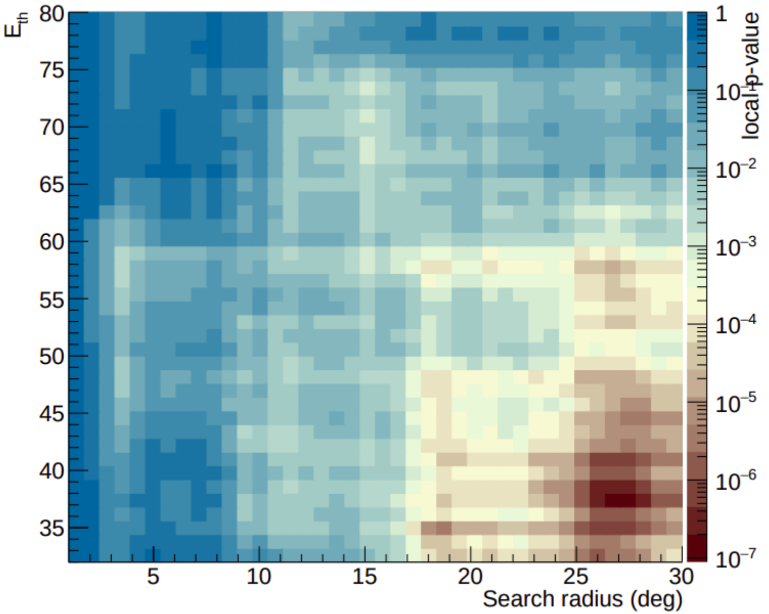

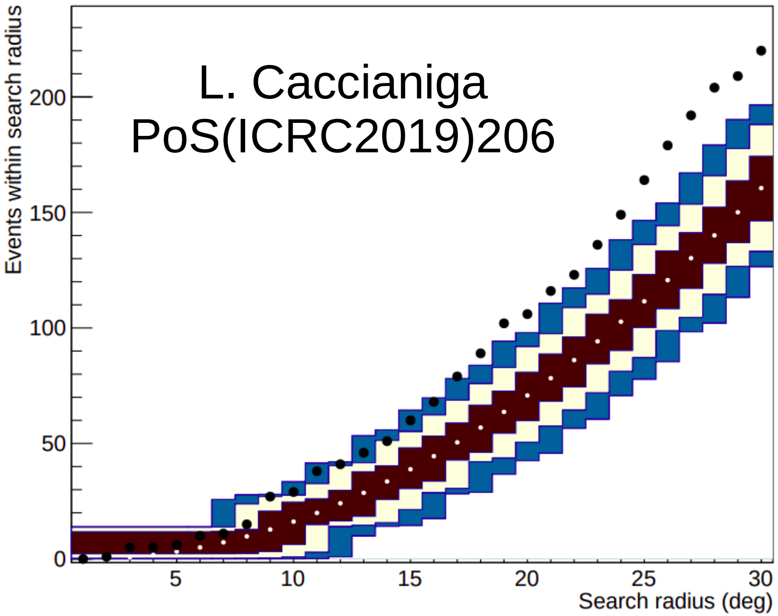

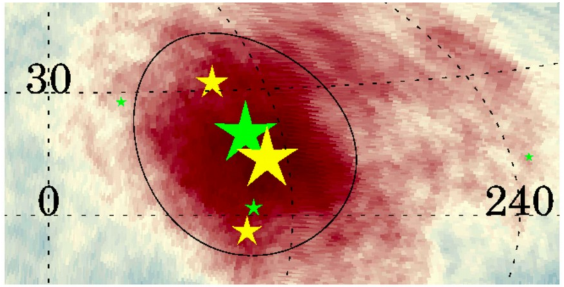

Most significant deviation from isotropy close to CEN-A

Scan in angular deviation and energy
→ **3.9 σ devation from isotropy**

Main results: composition

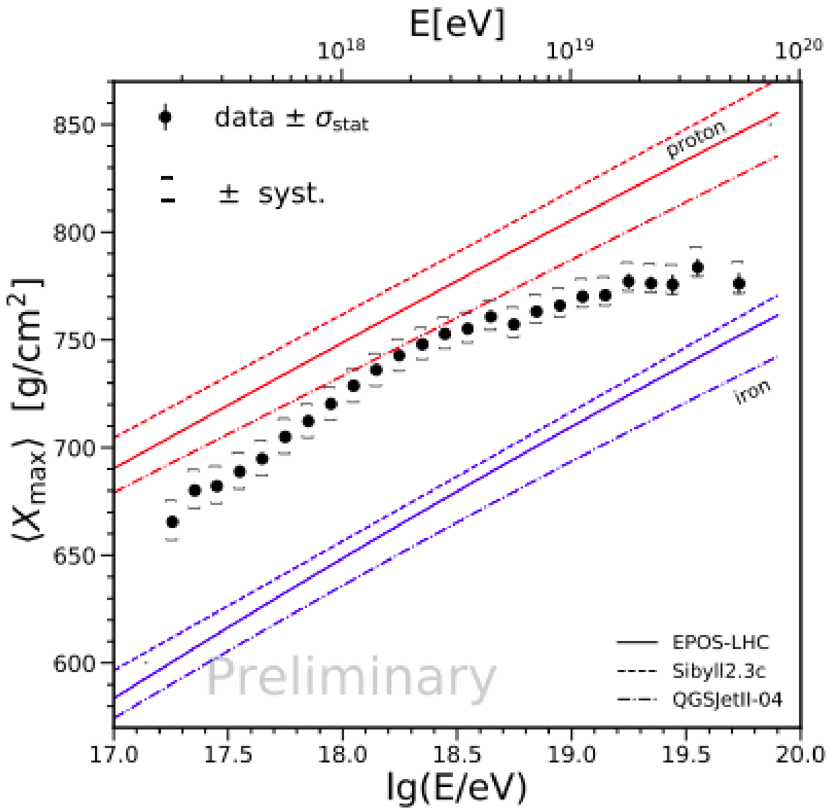

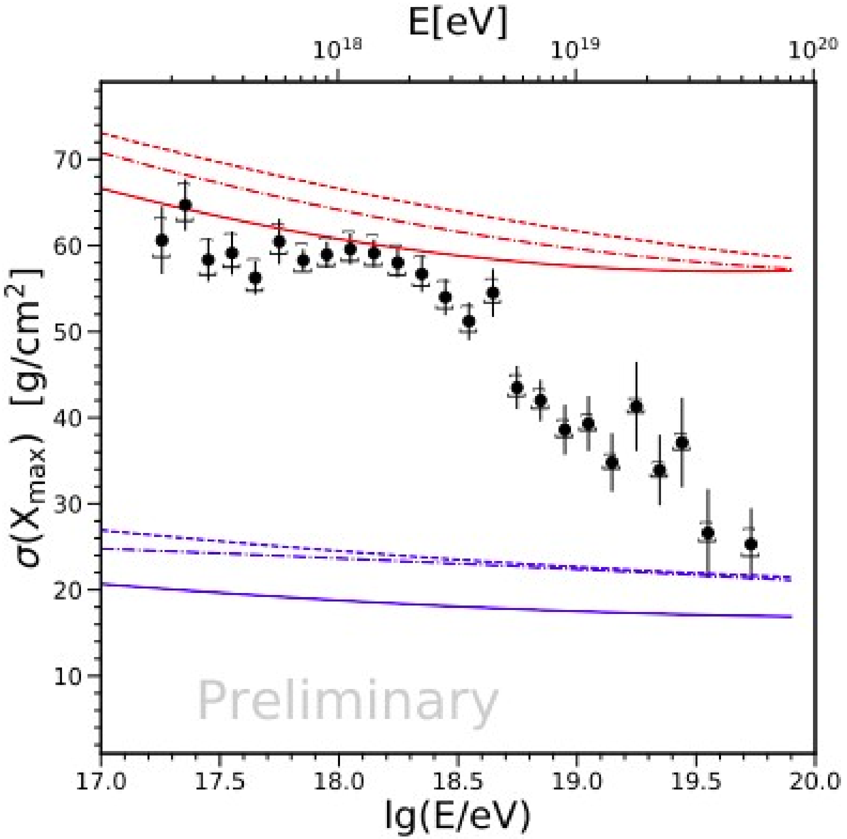

A. Yushkov
PoS(ICRC2019)482

- Getting lighter from 10^{17} to ~3×10^{18} eV
- Getting heavier above ~3×10^{18} eV

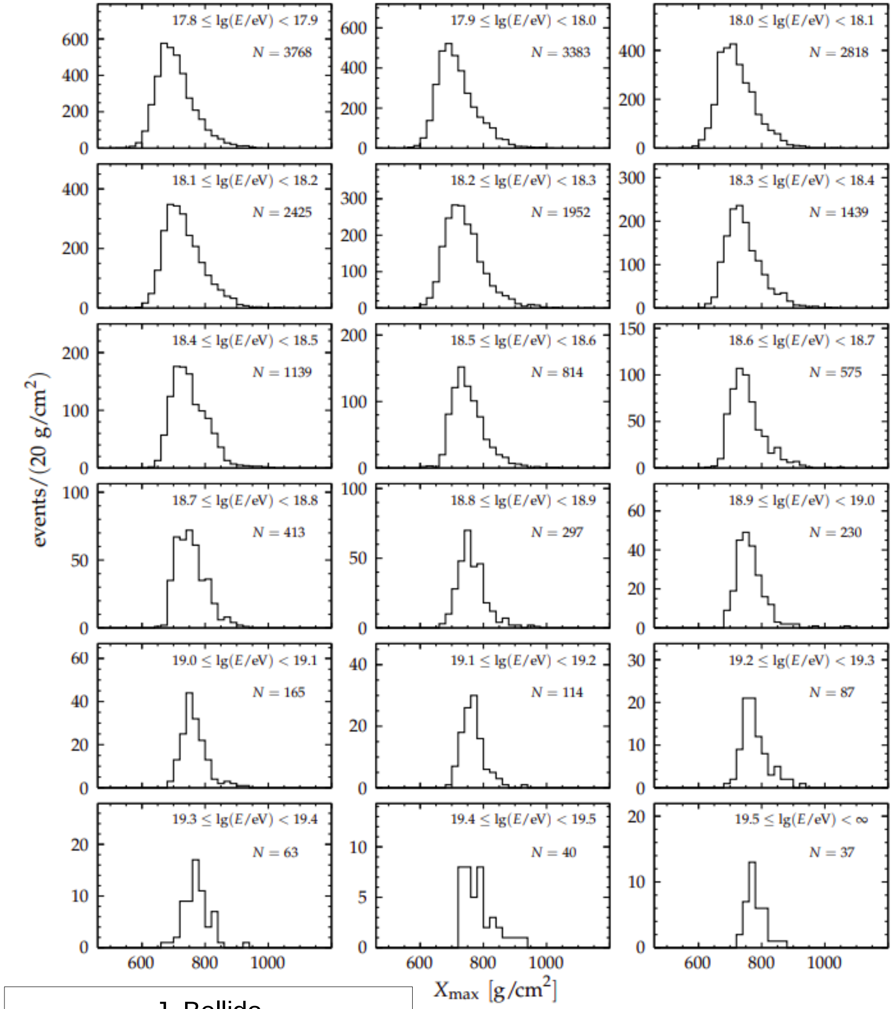

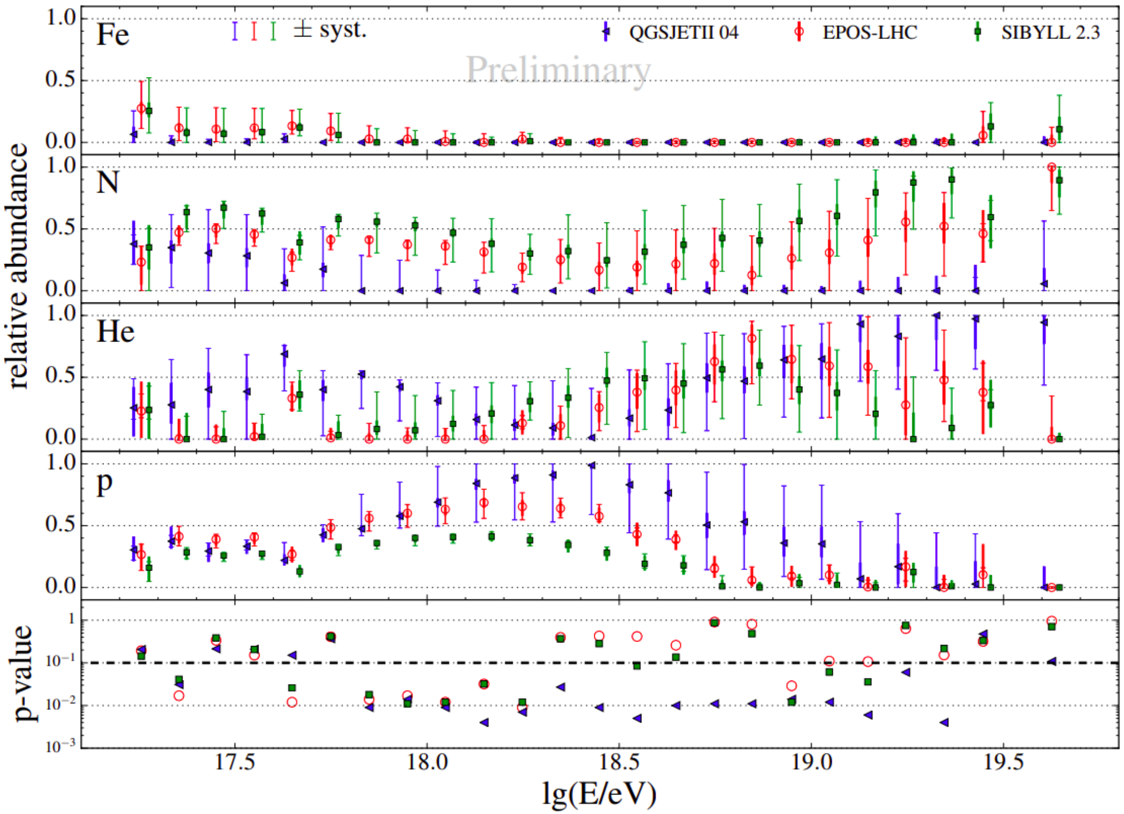

J. Bellido
PoS(ICRC2019)506

Phys. Rev. D90 122005 (2014)

- Iron component mostly absent (except at ~10^{17} eV)
- Getting lighter toward 10^{18} eV
- Getting heavier toward higher energies
- Mixed composition

Main results: neutrinos

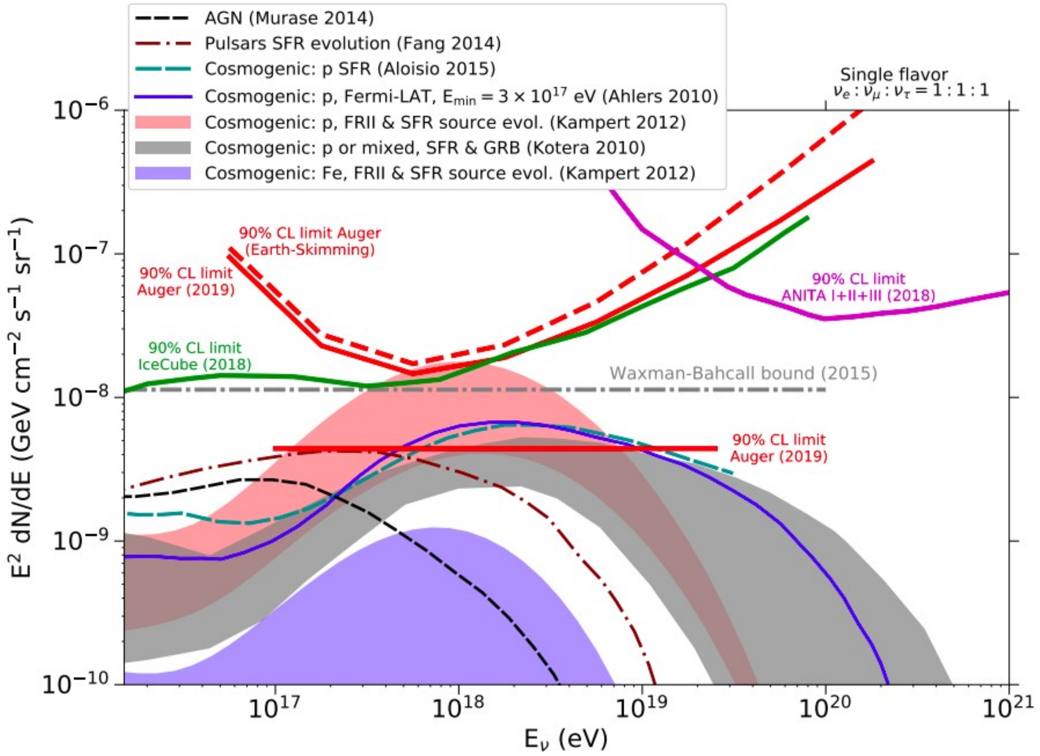

JCAP 10 (2019)022

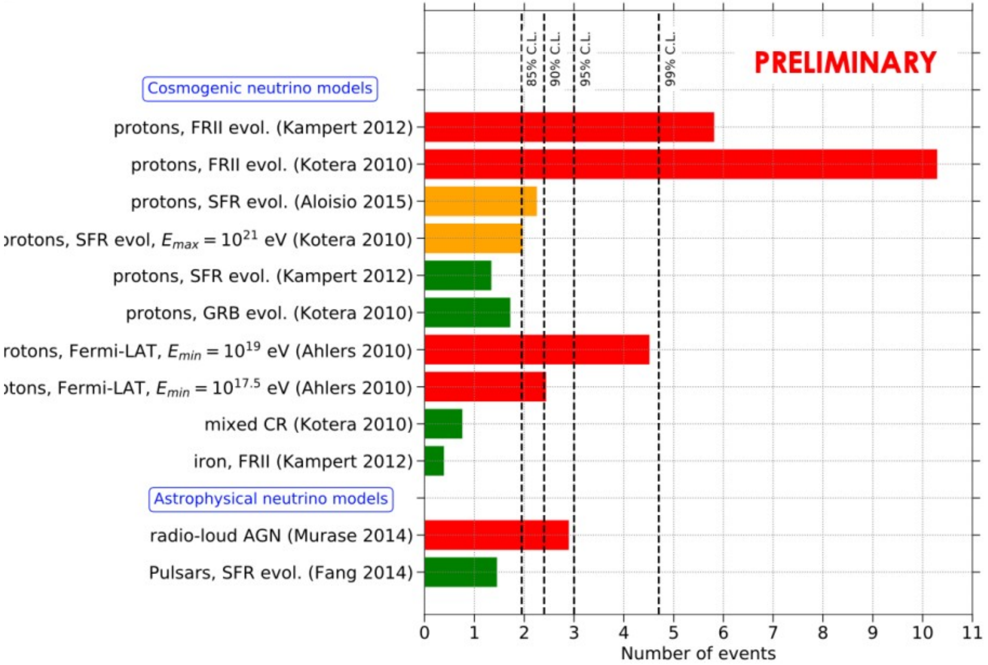

Diffuse neutrino limits exclude models dominated by light composition at sources

No point like source

No detection associated with transients

Main results: photons

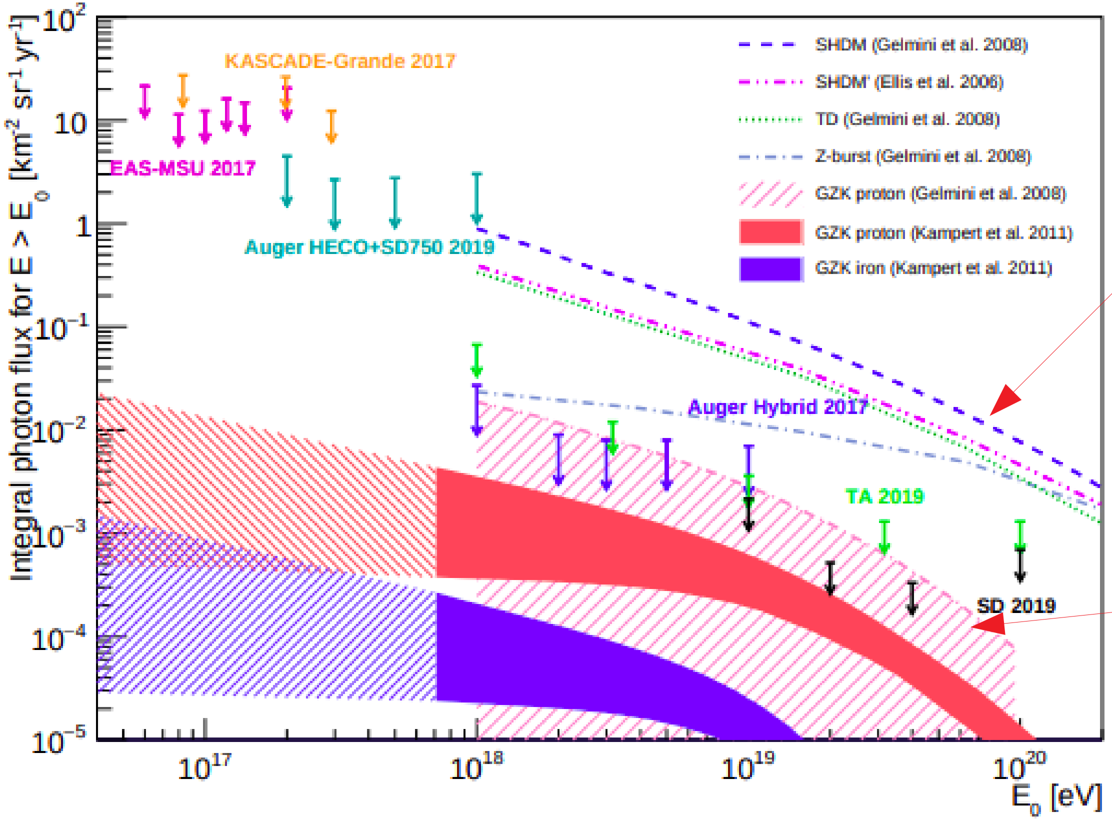

Photons limits exclude top-down CR production models

Light composition at the most extreme energies strongly constrained

$$p+\gamma_{CMB} \rightarrow \Delta^{+} \rightarrow p+\pi$$

$$\pi^0 \rightarrow 2\,\gamma$$

J. Rautenberg, PoS(ICRC2019)398

The energy spectrum of the Pierre Auger Observatory

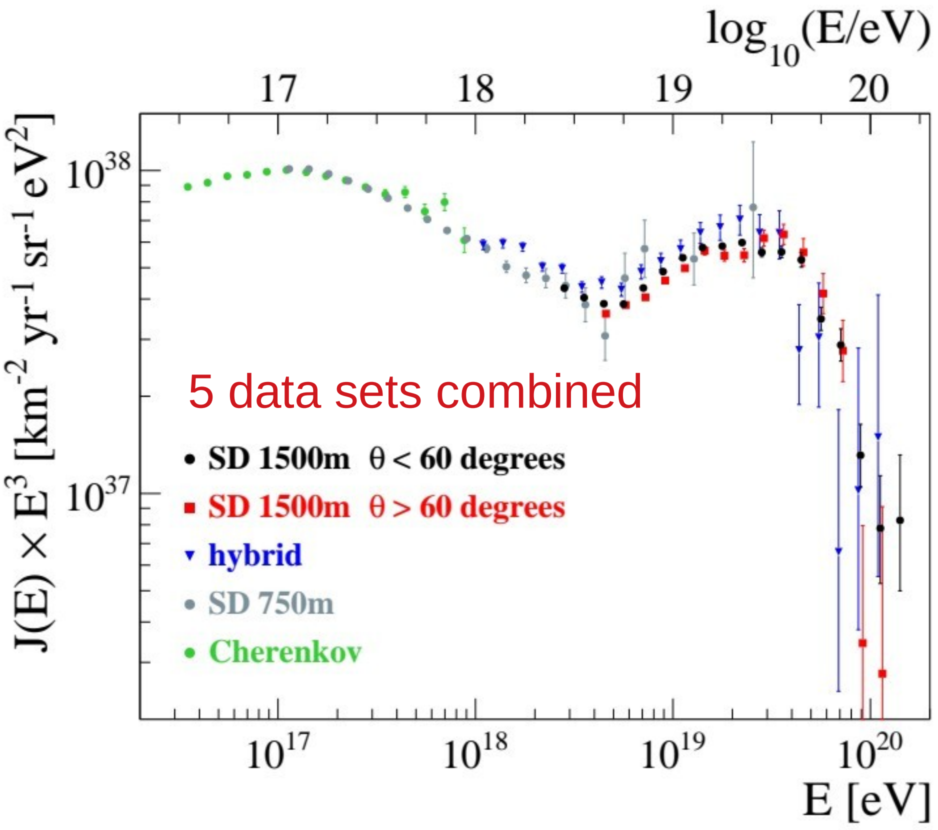

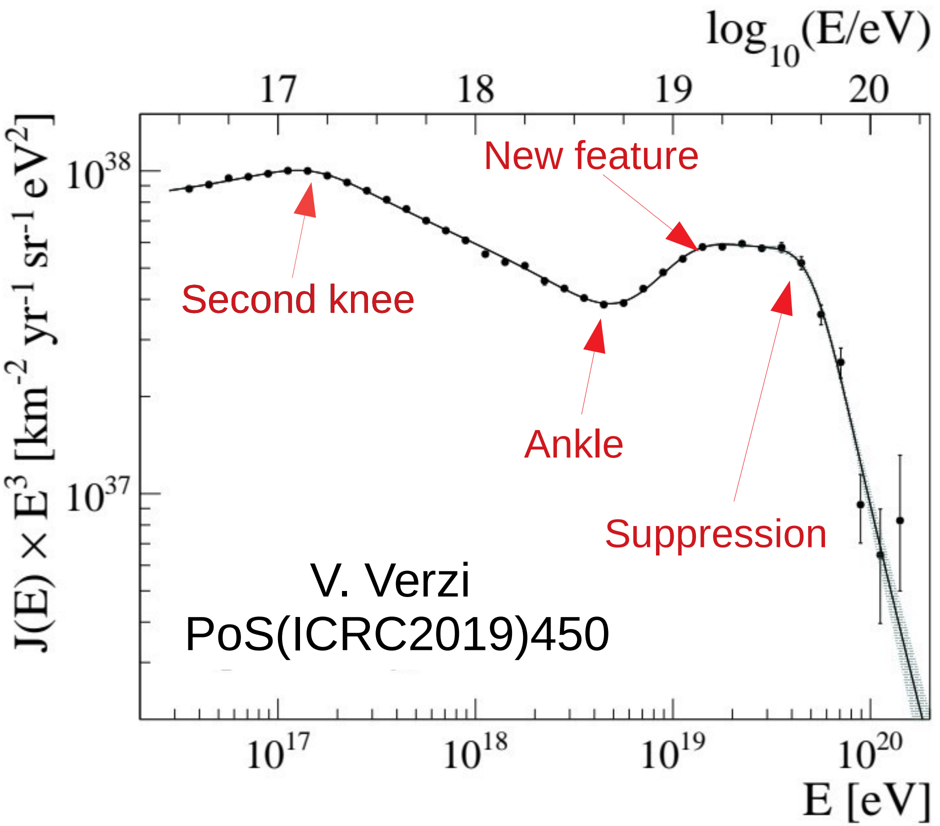

Spectrum measured over 4 orders of magnitude in energy

The Fluorescence Detector spectra

Problem of the FD shower geometry reconstruction:

correlation between the parameter of the formula

$$t_i = t_0 + \frac{R_p}{c} \tan\left(\frac{\chi_0 - \chi_i}{2}\right)$$

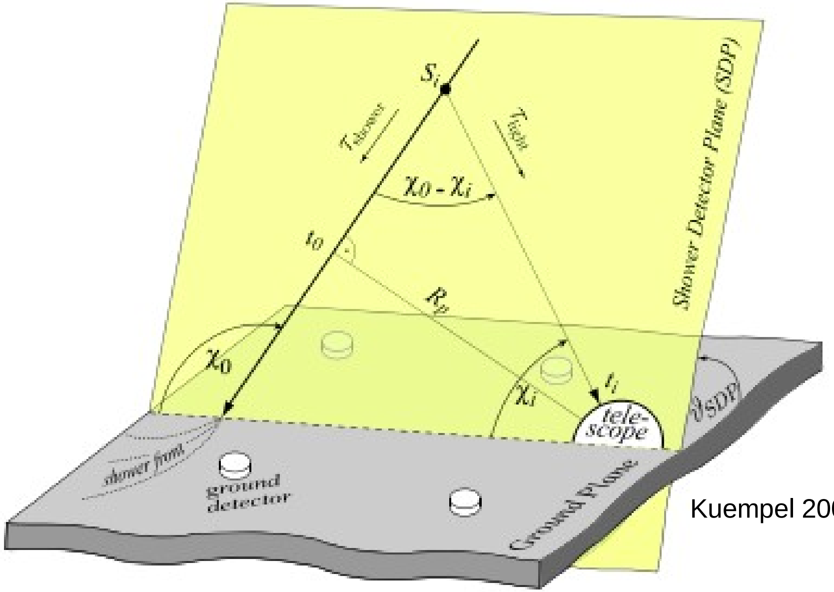

Kuempel 2008

Large systematics on the geometry reconstruction

Solution:

Coincident detection of one station on ground → **Hybrid spectrum**

Additional profile constrain on the shower geometry → **Cherenkov spectrum**

The Hybrid spectrum

$$E_0 = E_{cal} + E_{inv}$$

Primary

Calorimetric

Invisible

$$E_{cal} = \int \frac{dE}{dX} dX$$

Energy deposit

$$J_i = \frac{N_i}{\Delta E \; \mathcal{E}(E_i)}$$

Exposure $\mathcal{E}$ calculated with a full time-dependent events and detector response simulation

$$\mathcal{E}(E) = \int_t \int_\Omega \int_S \epsilon(E, t, \theta, \phi, x, y) \cos(\theta) \, dS \, d\Omega \, dt$$

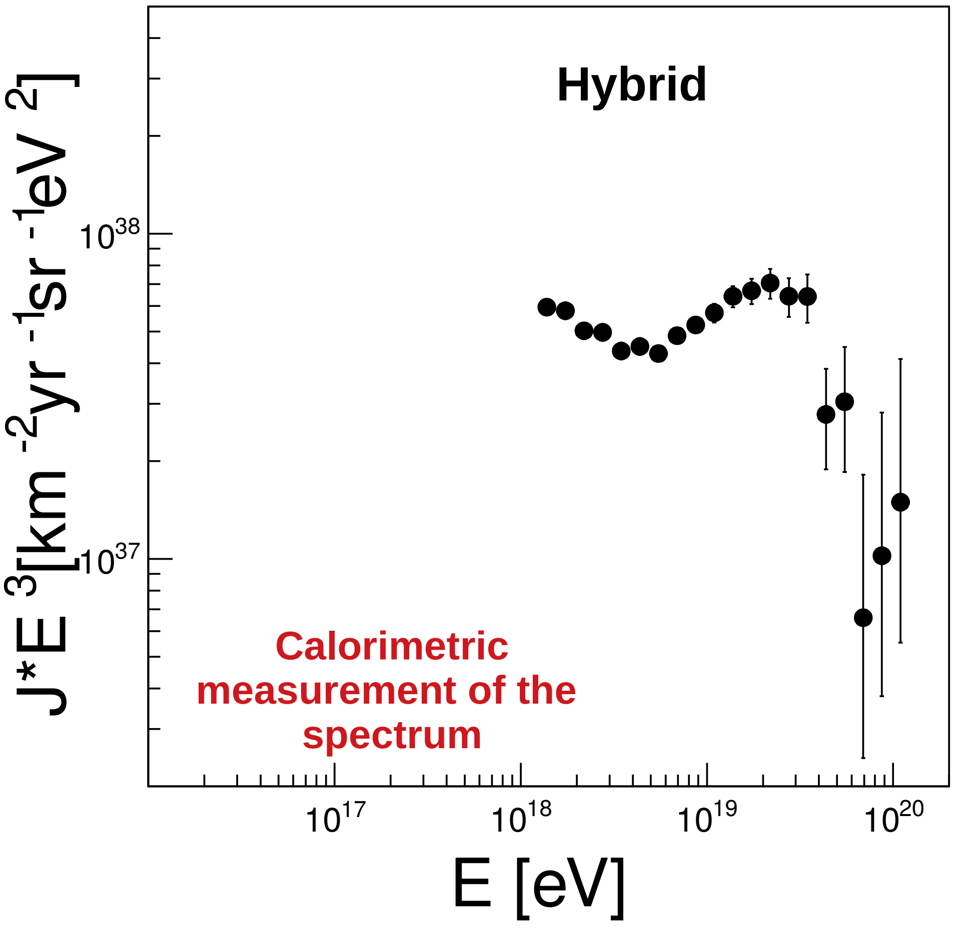

The Cherenkov spectrum

E > 10^{15} eV

Exposure: 2.86 km^2 sr yr @ 10^{17} eV

Small impact parameter (Large Cherenkov fraction)

Constrain on shower profile to reconstruct the geometry

1)Scan on χ_0

$$t_i = t_0 + \frac{R_p}{c} \tan\left(\frac{\chi_0 - \chi_i}{2}\right)$$

2)Linear regression to calculate R_p and t_0

3)Variate Gaisser-Hillas parameters to identify the best fit of the measured light profile

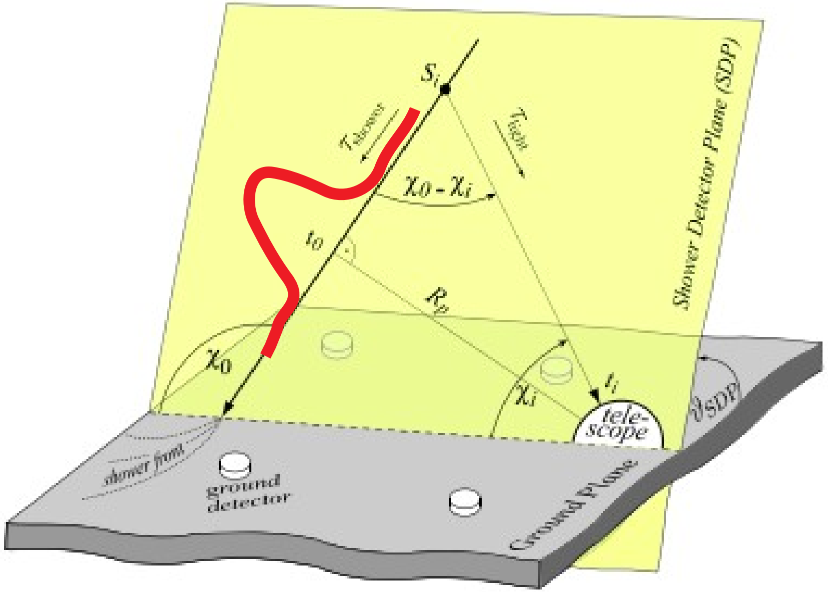

$$\frac{dE}{dX}(X) = \left(\frac{dE}{dX}\right)_{max} \left(\frac{X - X_0}{X_{max} - X_0}\right)^{\frac{X_{max} - X_0}{\lambda}} \exp \frac{X_{max} - X}{\lambda}$$

The Cherenkov spectrum

$$E_0 = E_{cal} + E_{inv}$$

Primary — Calorimetric — Invisible

$$E_{cal} = \int \frac{dE}{dX} dX$$

Energy deposit

$$J_i = \frac{N_i}{\Delta E \, \mathcal{E}(E_i)}$$

Exposure $\mathcal{E}$ calculated with a full time-dependent events and detector response simulation

Detector resolution effects corrected by forward folding procedure

Invisible energy extrapolated based on Ice-Top data

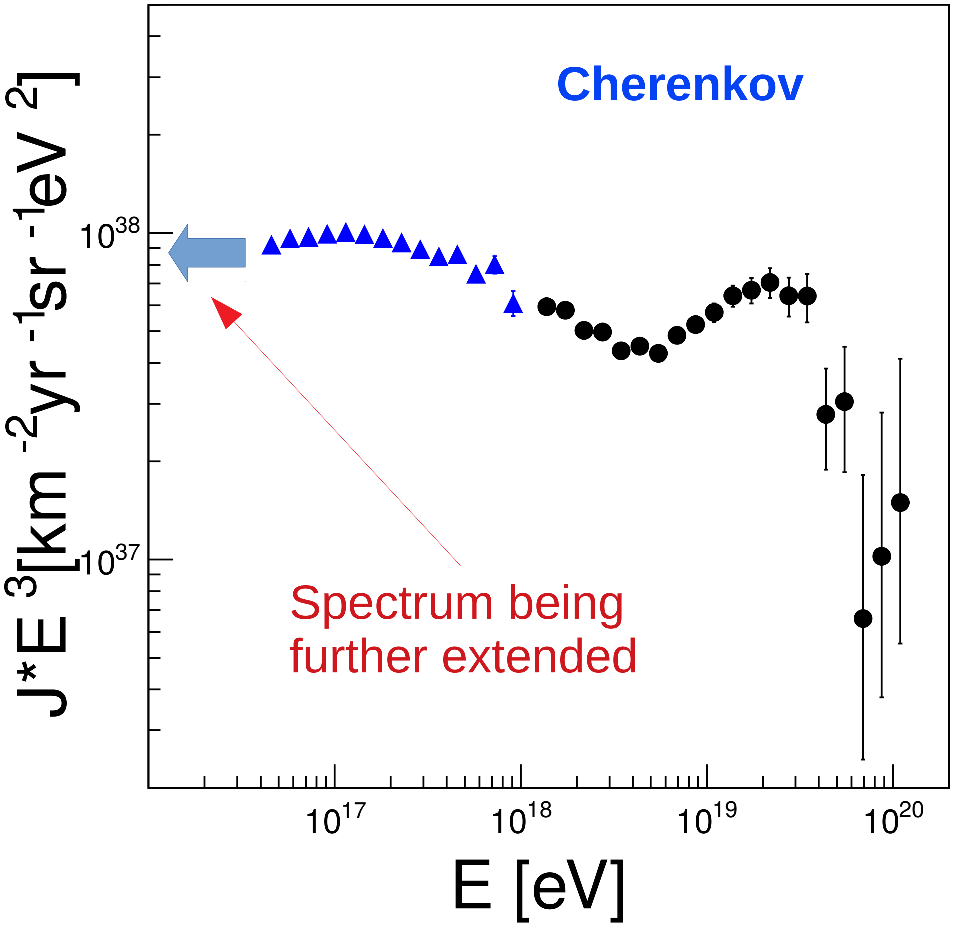

Invisible energy

Energy carried on ground by muons

$$E_0 = E_{cal} + E_{inv}$$

Primary

Calorimetric

Invisible

Main problem: Muon fraction at the highest energies strongly underestimated

Monte Carlo underestimates the invisible energy

Data driven estimation

By inclined events

By vertical events

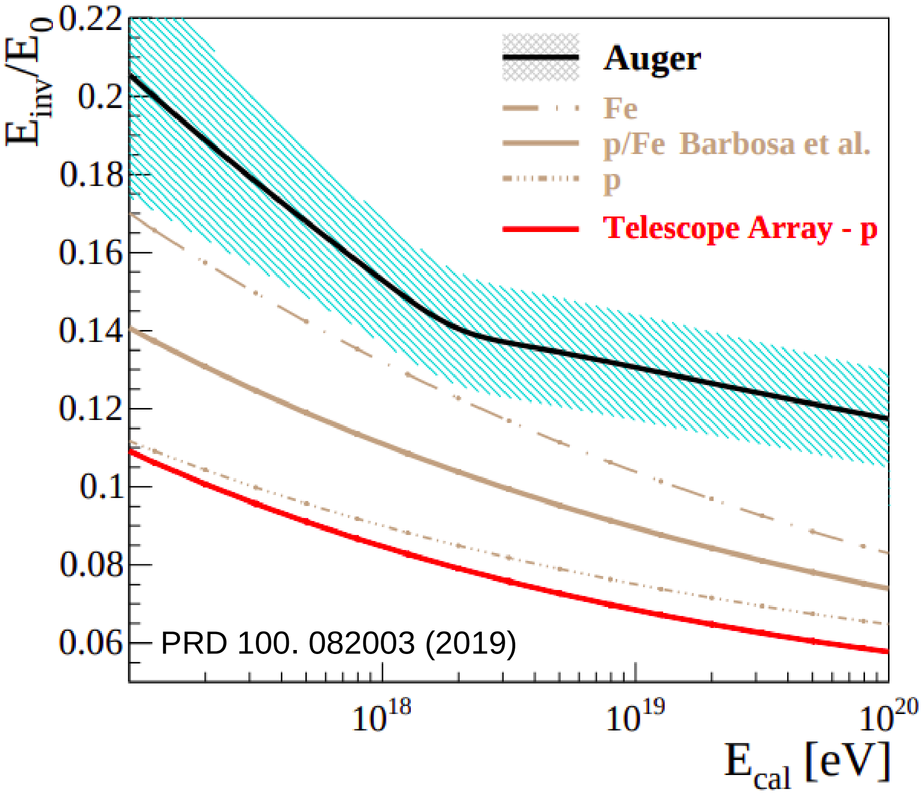

$$E_{inv} \propto N_\mu$$

$$E_{inv} = a\left(\frac{E_{cal}}{10^{18}\,eV}\right)^b$$

Forward folding procedure

Forward folding technique applied to correct for resolution effects

1) Calculate migration matrix
   a) Resolution
   b) Bias
   c) Efficiency

2) Fit of raw spectrum with detector effects

$$J^{raw}(E_{SD};s)=\frac{\int d\Omega\cos(\theta)\int dE\,\epsilon(E,\theta)J(E;s)k(E_{SD},E,\theta)}{\int d\Omega\cos(\theta)}$$

3) Calculation of correction factors c_i to apply on measured raw spectrum

$$c_i=\frac{\mu_i}{\nu_i}$$

μ_i: Expected rate in the i[th] bin without detector effects

ν_i: Expected rate in the i[th] bin with detector effects

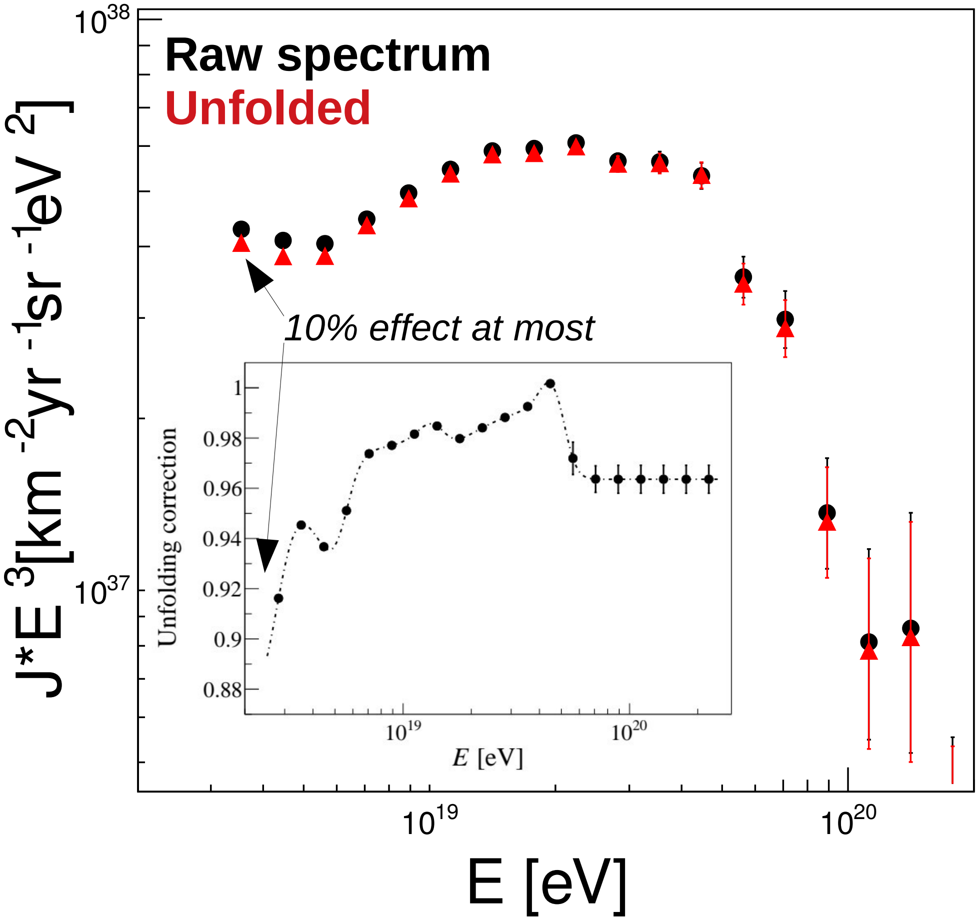

The Surface Detector spectrum

Largest exposure for cosmic rays

SD1500 spectrum:

Energy estimator (S)

0-60 degrees → **S(1000)**

60-80 degrees → **N_{19}**

SD750 spectrum → **S(450)**

Convert the estimator to an energy with a subset of hybrid events with SD and FD reconstruction

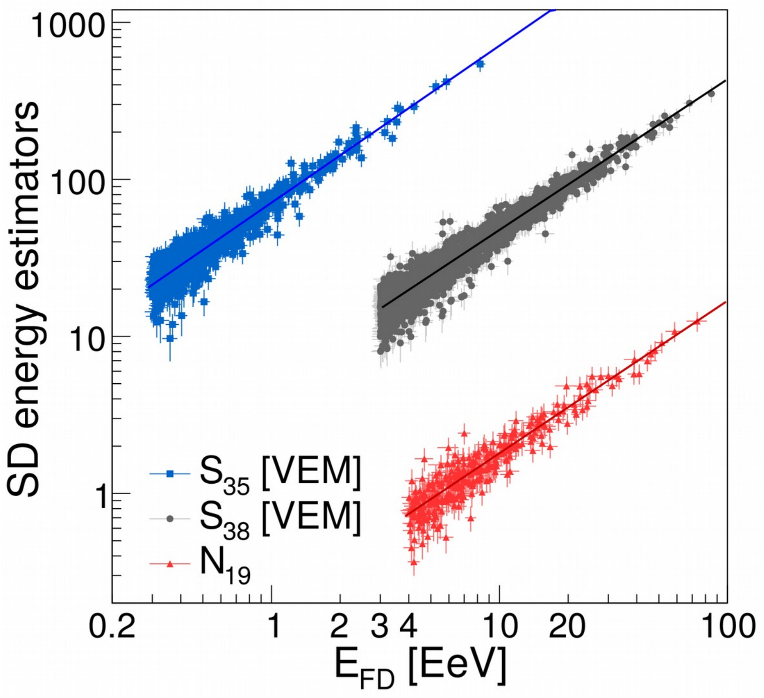

Energy scale is calorimetric

↓

Model independent determination of the energy

The Auger energy scale

1)define the energy estimator on all SD events
2)Fit the relation E_{FD} vs estimator on golden hybrids
3) SD energy: $E_{SD} = A\, S^B$

The SD energy estimators

For low zenith angle showers

Fit on the lateral distribution of the signal

Signal at the optimal distance from the core
(fluctuations are minimal at such distances)
1000 m for SD1500
450 m for SD750

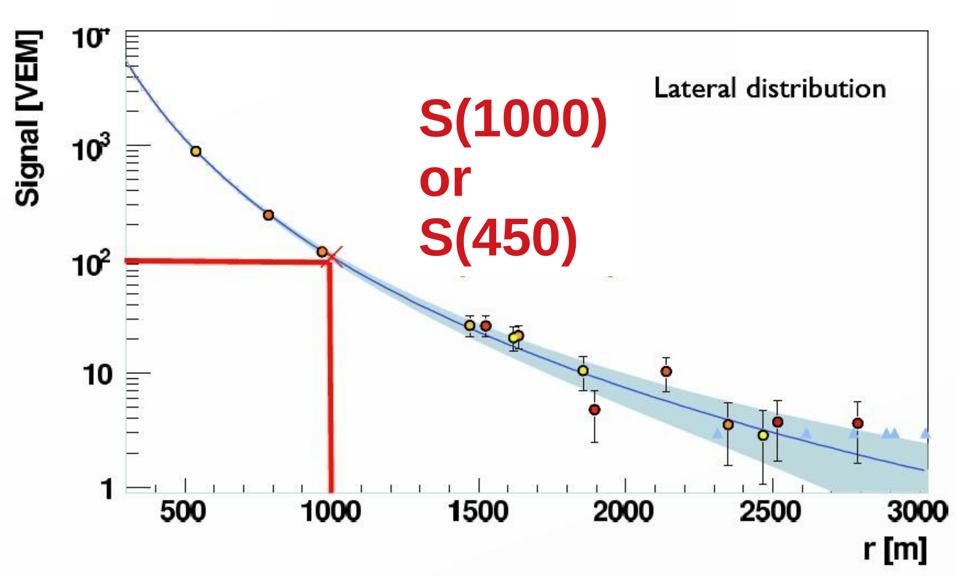

For high zenith angle showers (60-80°)

Fit distribution of secondary muons on ground
(shape of muon distribution universal)

$$\rho_\mu(\vec{r}) = N_{19}\,\rho_{\mu,19}(\vec{r},\theta,\phi)$$

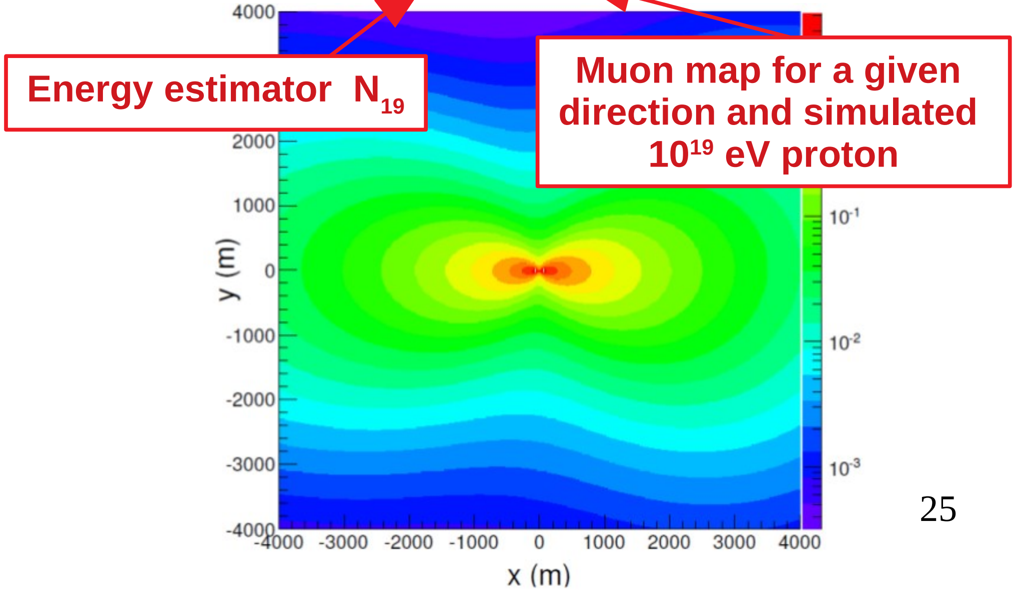

Correction of shower attenuation

The Constant Intensity Cut method

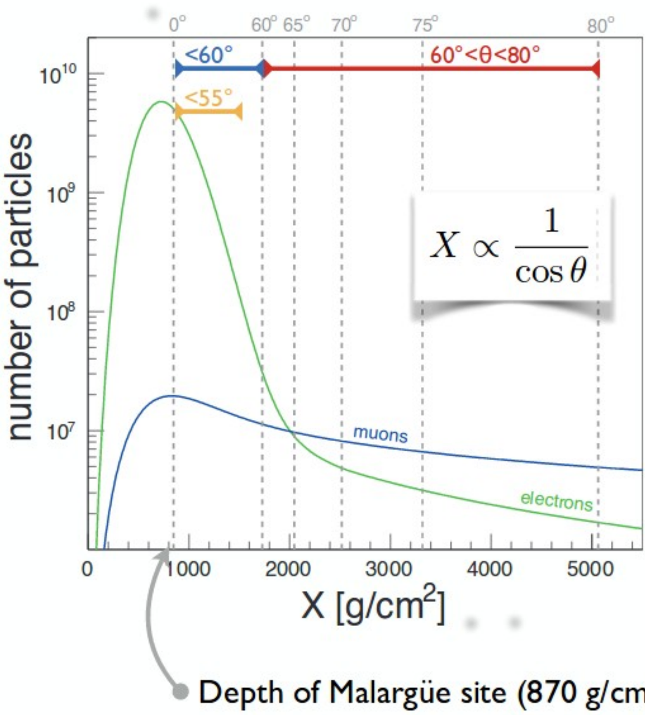

1)Isotropy in the arrival direction

2)Full efficiency

Showers of same energy arrive at the detector with same frequency independently of the direction

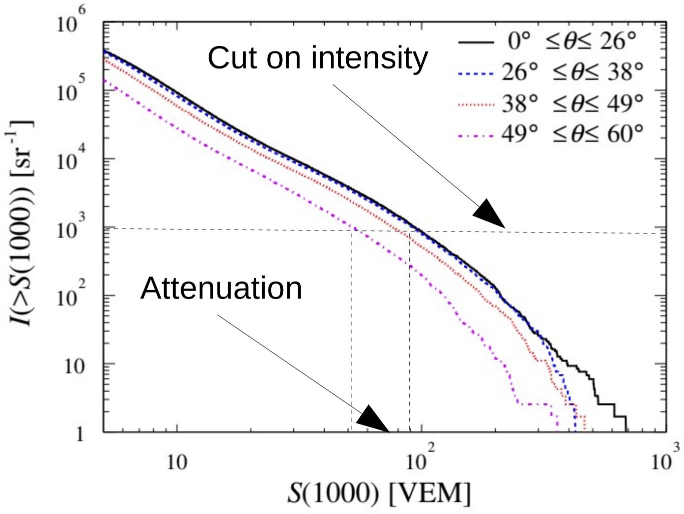

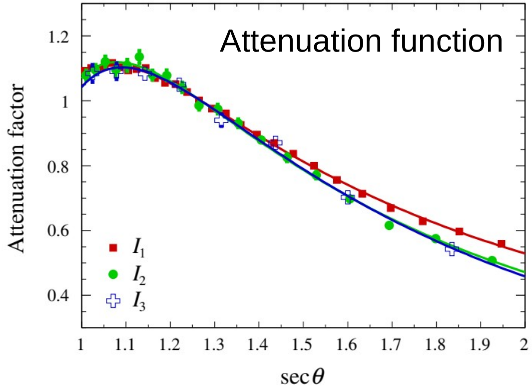

The shower size for fixed energy depends on the zenith angle

$S_{38} = S(1000) / f(\theta)$

$S_{35} = S(450) / f(\theta)$

The SD spectra

	SD1500 <60^{O}	SD1500 >60^{O}	SD750
Exposure [km^2 sr yr]	60425	17447	105.4
Threshold [eV]	$10^{18.4}$	$10^{18.6}$	10^{17}
Events	215030	24209	569285
ZA range [^{O}]	0-60	60-80	0-40
Energy estimator	S(1000) S_{38}	S(450) S_{35}	N_{19}

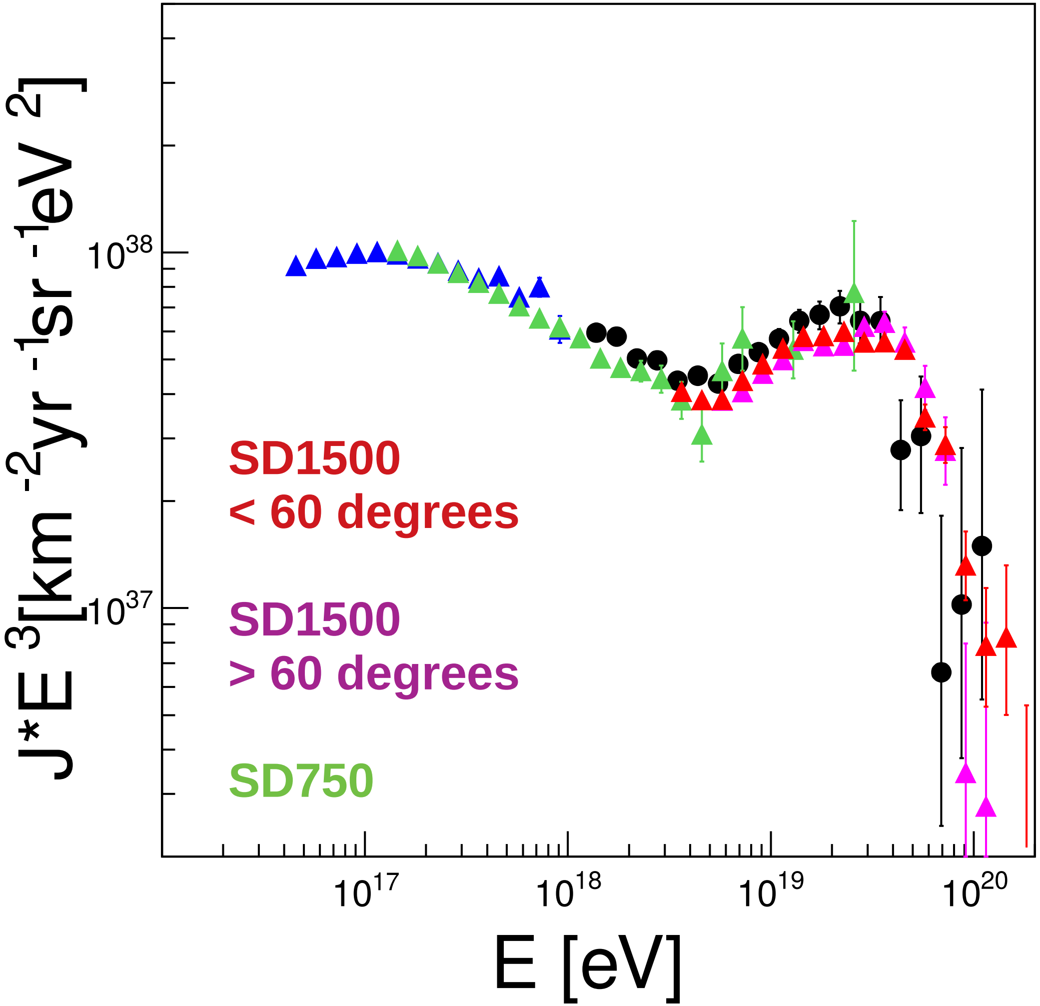

The combined spectrum

All the spectra can be combined to generate a single spectrum over 4 orders of magnitude

Maximum likelihood fit

$$L_k = L_{Poiss,k} * L_{d\epsilon,k} * L_{dE,k}$$

Additional constraint on the exposure

$$-2\ln L_\epsilon = \left(\frac{\delta\epsilon}{\epsilon}\right)^2$$

Additional constraint on the energy scale

$$-2\,lnL_{dE} = [\sigma^{-1}]_{AA}(\delta A)^2 + 2[\sigma^{-1}_{AB}]\,\delta A\,\delta B + [\sigma^{-1}]_{BB}(\delta B)^2$$

Weighted average of all the spectra

$$J = \frac{\Sigma_k J_k\, \mathcal{E}_k}{\Sigma_k\, \mathcal{E}_k}$$

(with k=Hybrid, Cherenkov, Vertical, Inclined, SD750)

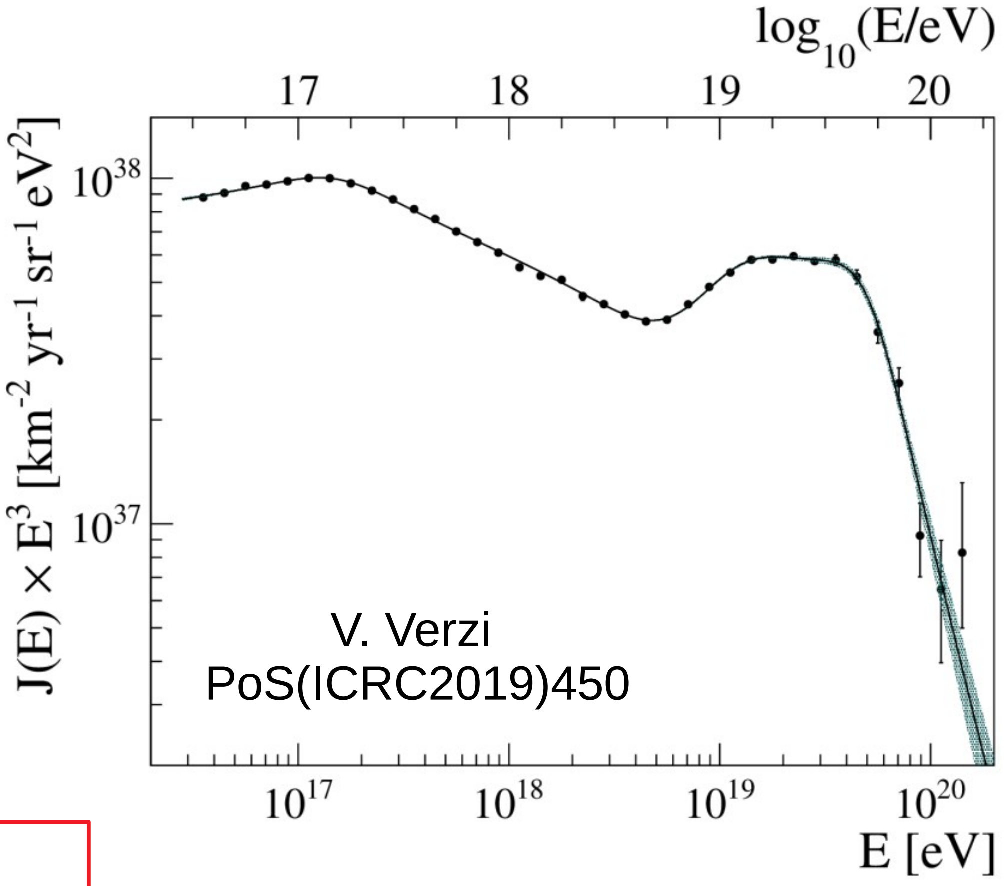

The SD-1500 spectrum

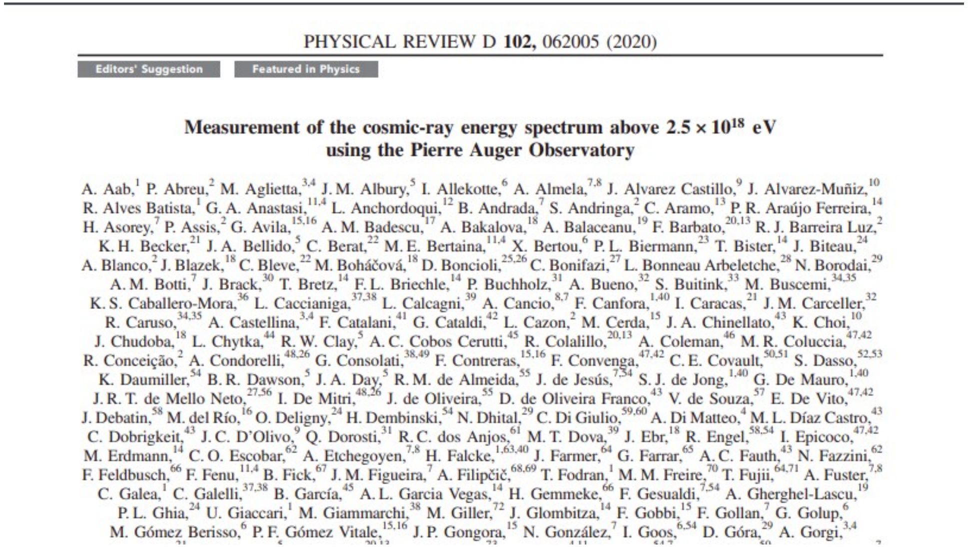

PHYSICAL REVIEW D 102, 062005 (2020)

Editors' Suggestion | Featured in Physics

Measurement of the cosmic-ray energy spectrum above 2.5×10^{18} eV using the Pierre Auger Observatory

A. Aab,[1] P. Abreu,[2] M. Aglietta,[3,4] J. M. Albury,[5] I. Allekotte,[6] A. Almela,[7,8] J. Alvarez Castillo,[9] J. Alvarez-Muñiz,[10] R. Alves Batista,[1] G. A. Anastasi,[11,4] L. Anchordoqui,[12] B. Andrada,[7] S. Andringa,[2] C. Aramo,[13] P. R. Araújo Ferreira,[14] H. Asorey,[7] P. Assis,[2] G. Avila,[15,16] A. M. Badescu,[17] A. Bakalova,[18] A. Balaceanu,[19] F. Barbato,[20,13] R. J. Barreira Luz,[2] K. H. Becker,[21] J. A. Bellido,[5] C. Berat,[22] M. E. Bertaina,[11,4] X. Bertou,[6] P. L. Biermann,[23] T. Bister,[14] J. Biteau,[24] A. Blanco,[2] J. Blazek,[18] C. Bleve,[22] M. Boháčová,[18] D. Boncioli,[25,26] C. Bonifazi,[27] L. Bonneau Arbeletche,[28] N. Borodai,[29] A. M. Botti,[7] J. Brack,[30] T. Bretz,[14] F. L. Briechle,[14] P. Buchholz,[31] A. Bueno,[32] S. Buitink,[33] M. Buscemi,[34,35] K. S. Caballero-Mora,[36] L. Caccianiga,[37,38] L. Calcagni,[39] A. Cancio,[8,7] F. Canfora,[1,40] I. Caracas,[21] J. M. Carceller,[32] R. Caruso,[34,35] A. Castellina,[3,4] F. Catalani,[41] G. Cataldi,[42] L. Cazon,[2] M. Cerda,[15] J. A. Chinellato,[43] K. Choi,[10] J. Chudoba,[18] L. Chytka,[44] R. W. Clay,[5] A. C. Cobos Cerutti,[45] R. Colalillo,[20,13] A. Coleman,[46] M. R. Coluccia,[47,42] R. Conceição,[2] A. Condorelli,[48,26] G. Consolati,[38,49] F. Contreras,[15,16] F. Convenga,[47,42] C. E. Covault,[50,51] S. Dasso,[52,53] K. Daumiller,[54] B. R. Dawson,[5] J. A. Day,[5] R. M. de Almeida,[55] J. de Jesús,[7,54] S. J. de Jong,[1,40] G. De Mauro,[1,40] J. R. T. de Mello Neto,[27,56] I. De Mitri,[48,26] J. de Oliveira,[55] D. de Oliveira Franco,[43] V. de Souza,[57] E. De Vito,[47,42] J. Debatin,[58] M. del Río,[16] O. Deligny,[24] H. Dembinski,[54] N. Dhital,[29] C. Di Giulio,[59,60] A. Di Matteo,[4] M. L. Díaz Castro,[43] C. Dobrigkeit,[43] J. C. D'Olivo,[9] Q. Dorosti,[31] R. C. dos Anjos,[61] M. T. Dova,[39] J. Ebr,[18] R. Engel,[58,54] I. Epicoco,[47,42] M. Erdmann,[14] C. O. Escobar,[62] A. Etchegoyen,[7,8] H. Falcke,[1,63,40] J. Farmer,[64] G. Farrar,[65] A. C. Fauth,[43] N. Fazzini,[62] F. Feldbusch,[66] F. Fenu,[11,4] B. Fick,[67] J. M. Figueira,[7] A. Filipčič,[68,69] T. Fodran,[1] M. M. Freire,[70] T. Fujii,[64,71] A. Fuster,[7,8] C. Galea,[1] C. Galelli,[37,38] B. García,[45] A. L. Garcia Vegas,[14] H. Gemmeke,[66] F. Gesualdi,[7,54] A. Gherghel-Lascu,[19] P. L. Ghia,[24] U. Giaccari,[1] M. Giammarchi,[38] M. Giller,[72] J. Glombitza,[14] F. Gobbi,[15] F. Gollan,[7] G. Golup,[6] M. Gómez Berisso,[6] P. F. Gómez Vitale,[15,16] J. P. Gongora,[15] N. González,[7] I. Goos,[6,54] D. Góra,[29] A. Gorgi,[3,4]

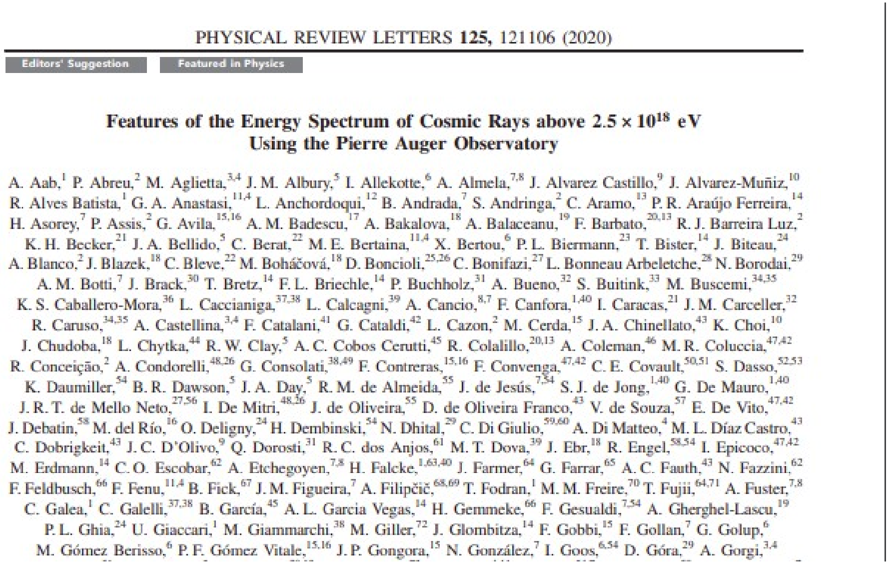

PHYSICAL REVIEW LETTERS 125, 121106 (2020)

Editors' Suggestion | Featured in Physics

Features of the Energy Spectrum of Cosmic Rays above 2.5×10^{18} eV Using the Pierre Auger Observatory

A. Aab,[1] P. Abreu,[2] M. Aglietta,[3,4] J. M. Albury,[5] I. Allekotte,[6] A. Almela,[7,8] J. Alvarez Castillo,[9] J. Alvarez-Muñiz,[10] R. Alves Batista,[1] G. A. Anastasi,[11,4] L. Anchordoqui,[12] B. Andrada,[7] S. Andringa,[2] C. Aramo,[13] P. R. Araújo Ferreira,[14] H. Asorey,[7] P. Assis,[2] G. Avila,[15,16] A. M. Badescu,[17] A. Bakalova,[18] A. Balaceanu,[19] F. Barbato,[20,13] R. J. Barreira Luz,[2] K. H. Becker,[21] J. A. Bellido,[5] C. Berat,[22] M. E. Bertaina,[11,4] X. Bertou,[6] P. L. Biermann,[23] T. Bister,[14] J. Biteau,[24] A. Blanco,[2] J. Blazek,[18] C. Bleve,[22] M. Boháčová,[18] D. Boncioli,[25,26] C. Bonifazi,[27] L. Bonneau Arbeletche,[28] N. Borodai,[29] A. M. Botti,[7] J. Brack,[30] T. Bretz,[14] F. L. Briechle,[14] P. Buchholz,[31] A. Bueno,[32] S. Buitink,[33] M. Buscemi,[34,35] K. S. Caballero-Mora,[36] L. Caccianiga,[37,38] L. Calcagni,[39] A. Cancio,[8,7] F. Canfora,[1,40] I. Caracas,[21] J. M. Carceller,[32] R. Caruso,[34,35] A. Castellina,[3,4] F. Catalani,[41] G. Cataldi,[42] L. Cazon,[2] M. Cerda,[15] J. A. Chinellato,[43] K. Choi,[10] J. Chudoba,[18] L. Chytka,[44] R. W. Clay,[5] A. C. Cobos Cerutti,[45] R. Colalillo,[20,13] A. Coleman,[46] M. R. Coluccia,[47,42] R. Conceição,[2] A. Condorelli,[48,26] G. Consolati,[38,49] F. Contreras,[15,16] F. Convenga,[47,42] C. E. Covault,[50,51] S. Dasso,[52,53] K. Daumiller,[54] B. R. Dawson,[5] J. A. Day,[5] R. M. de Almeida,[55] J. de Jesús,[7,54] S. J. de Jong,[1,40] G. De Mauro,[1,40] J. R. T. de Mello Neto,[27,56] I. De Mitri,[48,26] J. de Oliveira,[55] D. de Oliveira Franco,[43] V. de Souza,[57] E. De Vito,[47,42] J. Debatin,[58] M. del Río,[16] O. Deligny,[24] H. Dembinski,[54] N. Dhital,[29] C. Di Giulio,[59,60] A. Di Matteo,[4] M. L. Díaz Castro,[43] C. Dobrigkeit,[43] J. C. D'Olivo,[9] Q. Dorosti,[31] R. C. dos Anjos,[61] M. T. Dova,[39] J. Ebr,[18] R. Engel,[58,54] I. Epicoco,[47,42] M. Erdmann,[14] C. O. Escobar,[62] A. Etchegoyen,[7,8] H. Falcke,[1,63,40] J. Farmer,[64] G. Farrar,[65] A. C. Fauth,[43] N. Fazzini,[62] F. Feldbusch,[66] F. Fenu,[11,4] B. Fick,[67] J. M. Figueira,[7] A. Filipčič,[68,69] T. Fodran,[1] M. M. Freire,[70] T. Fujii,[64,71] A. Fuster,[7,8] C. Galea,[1] C. Galelli,[37,38] B. García,[45] A. L. Garcia Vegas,[14] H. Gemmeke,[66] F. Gesualdi,[7,54] A. Gherghel-Lascu,[19] P. L. Ghia,[24] U. Giaccari,[1] M. Giammarchi,[38] M. Giller,[72] J. Glombitza,[14] F. Gobbi,[15] F. Gollan,[7] G. Golup,[6] M. Gómez Berisso,[6] P. F. Gómez Vitale,[15,16] J. P. Gongora,[15] N. González,[7] I. Goos,[6,54] D. Góra,[29] A. Gorgi,[3,4]

Most precise estimate of the spectrum done above 2.5×10^{18} eV

Spectrum free of assumptions on hadronic interactions or composition

Data driven E_{SD} resolution

$$\kappa(E_{SD}|E;\theta) = \frac{1}{\sqrt{2\pi}\sigma_{SD}(E,\theta)} \times \exp\left[-\frac{(E_{SD} - E(1+b_{SD}(E,\theta)))^2}{2\sigma_{SD}^2(E,\theta)}\right]$$

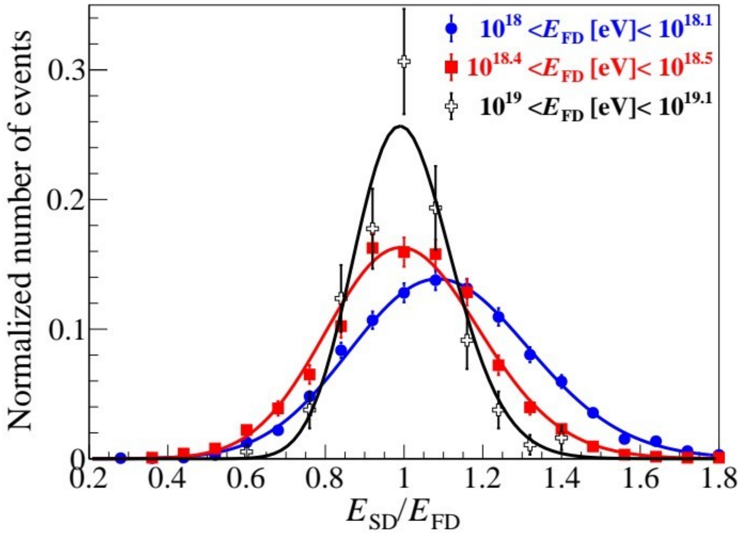

Resolution from E_{SD} / E_{FD} ratio (not from MC)

E_{SD} / E_{FD} follows a Gaussian ratio distribution (With σ_{FD} ~ 7-8%)

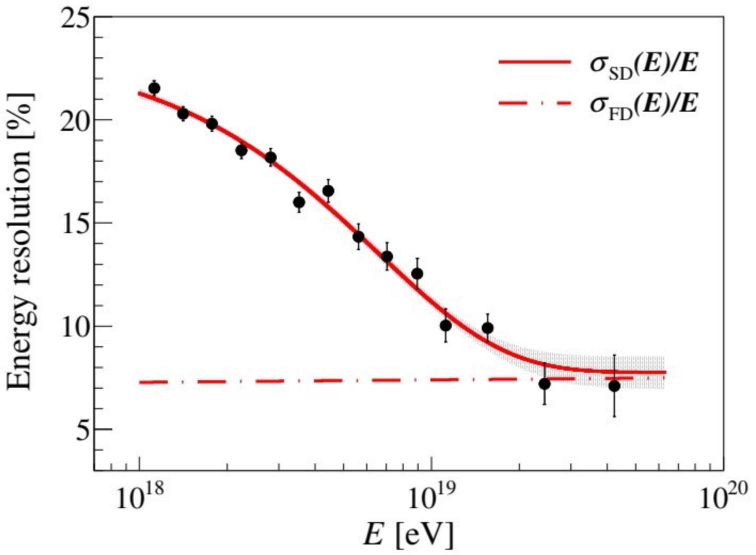

$$\frac{\sigma_{SD}(E)}{E} = \sigma_0 + \sigma_1 \exp\left(-\frac{E}{E_\sigma}\right)$$

Data driven E_{SD} bias

A bias appears under threshold:

- Statistical bias (upward fluctuation triggers)
- Mass selection bias

$$\kappa(E_{\rm SD}|E;\theta) = \frac{1}{\sqrt{2\pi}\sigma_{\rm SD}(E,\theta)} \times \exp\left[-\frac{(E_{\rm SD} - E(1 + b_{\rm SD}(E,\theta)))^2}{2\sigma^2_{\rm SD}(E,\theta)}\right]$$

Bias strongly zenith angle dependent

$$b_{\rm SD}(E,\theta) = (b_0 + b_1 \exp(-\lambda_b(\cos\theta - 0.5)))\log_{10}\left(\frac{E_*}{E}\right)$$

No bias above threshold (2.5×10^18 eV)

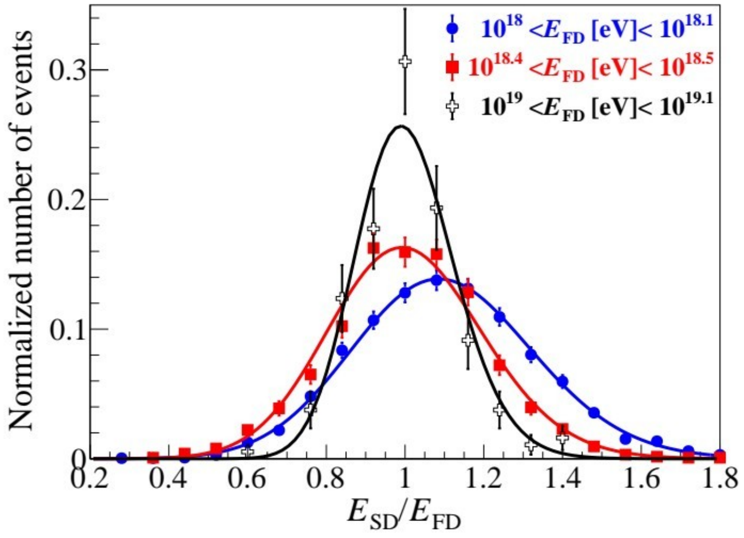

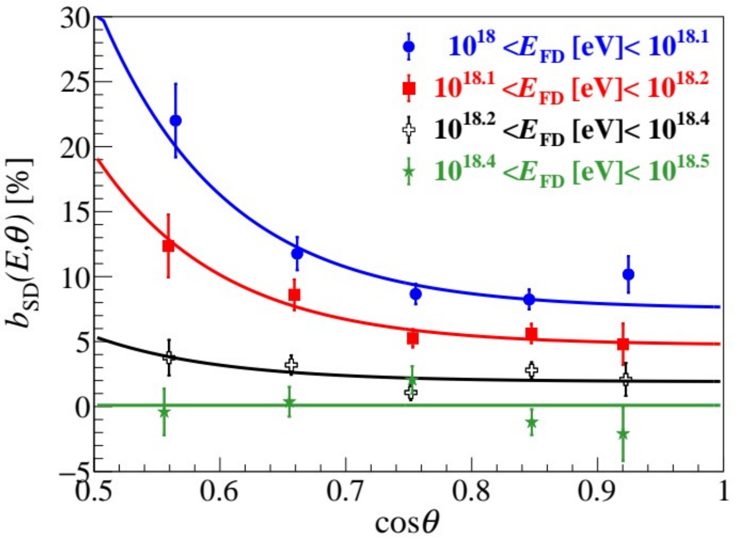

Data driven E_{SD} efficiency

Hybrid sample has lower threshold than Surface Detector

Efficiency can be calculated as a function of FD energy

Full efficiency around 2.5×10^{18} eV

$$\epsilon(E,\theta) = \frac{1}{2}\left[1 + \text{erf}\left(\frac{\log_{10}(E/\text{eV}) - p_0(\theta)}{p_1}\right)\right]$$

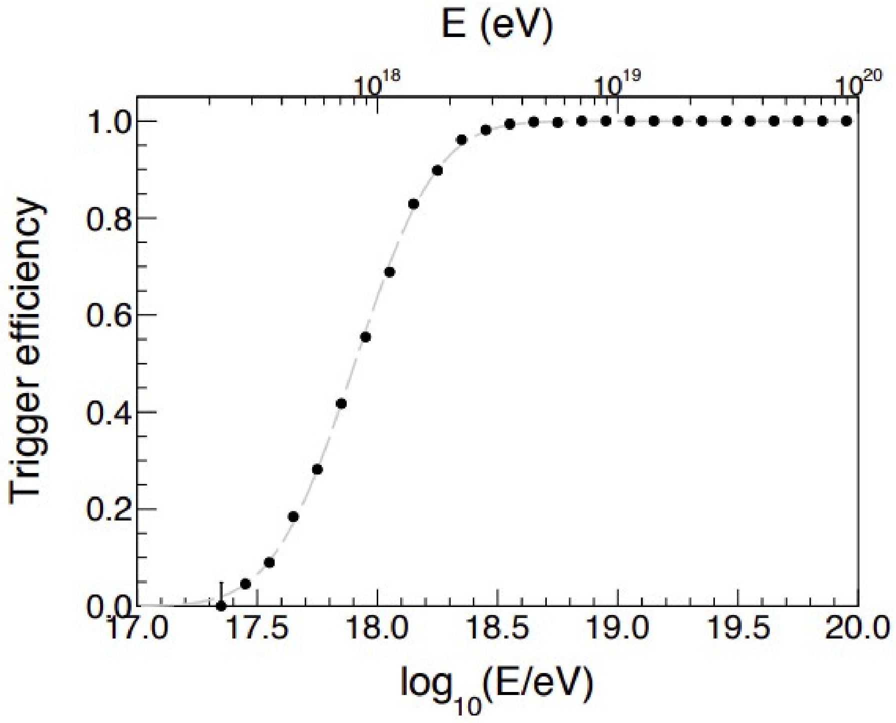

Energy dependent CIC

Attenuation function changes with energy (Muonic fraction and energy change with energy)

Statistics is now sufficient to account for such evolution

$$S_{38} = S(1000)/(1 + a X + b X^2 + c X^3)$$

$$X = \cos^2(\theta) - \cos^2(38^o)$$

$$\begin{cases} a(S) = a_0 + a_1 * y + a_2 * y^2 \\ b(S) = b_0 + b_1 * y + b_2 * y^2 \\ c(S) = c_0 + c_1 * y + c_2 * y^2 \end{cases}$$

$$y = \log_{10}(S_{38}/40\,VEM)$$

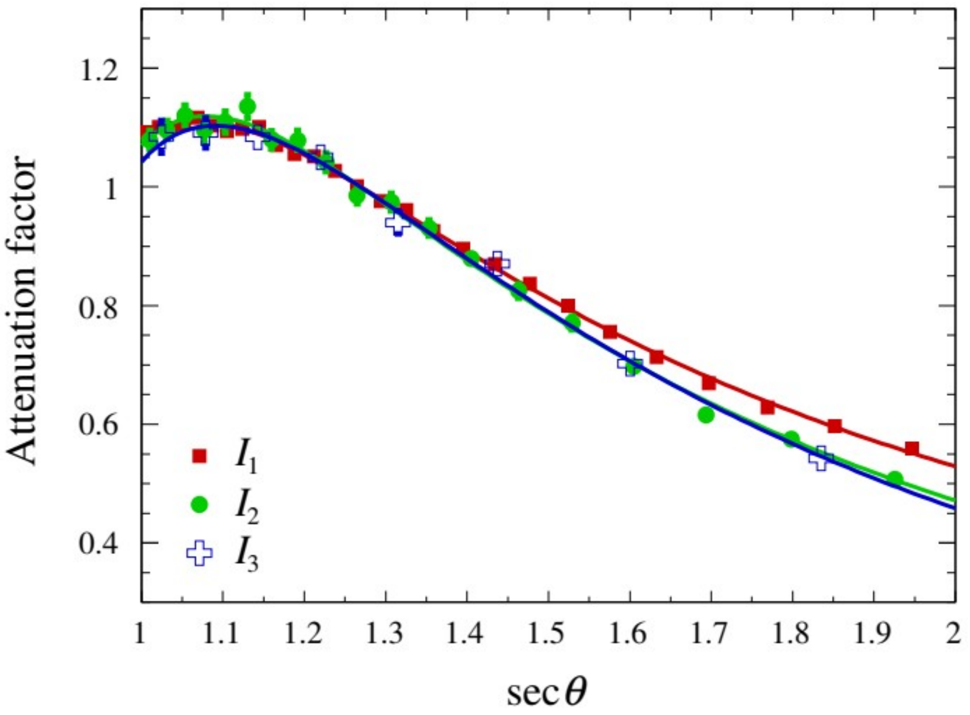

Spectral features

TABLE III. Best-fit parameters, with statistical and systematic uncertainties, for the energy spectrum measured at the Pierre Auger Observatory.

parameter	value $\pm\sigma_{\text{stat}} \pm \sigma_{\text{sys.}}$
J_0 [km^{-2} sr^{-1} yr^{-1} eV^{-1}]	$(1.315 \pm 0.004 \pm 0.400) \times 10^{-18}$
γ_1	$3.29 \pm 0.02 \pm 0.10$
γ_2	$2.51 \pm 0.03 \pm 0.05$
γ_3	$3.05 \pm 0.05 \pm 0.10$
γ_4	$5.1 \pm 0.3 \pm 0.1$
E_{12} [eV] (ankle)	$(5.0 \pm 0.1 \pm 0.8) \times 10^{18}$
E_{23} [eV]	$(13 \pm 1 \pm 2) \times 10^{18}$
E_{34} [eV] (suppression)	$(46 \pm 3 \pm 6) \times 10^{18}$
D/n_{dof}	17.0/12

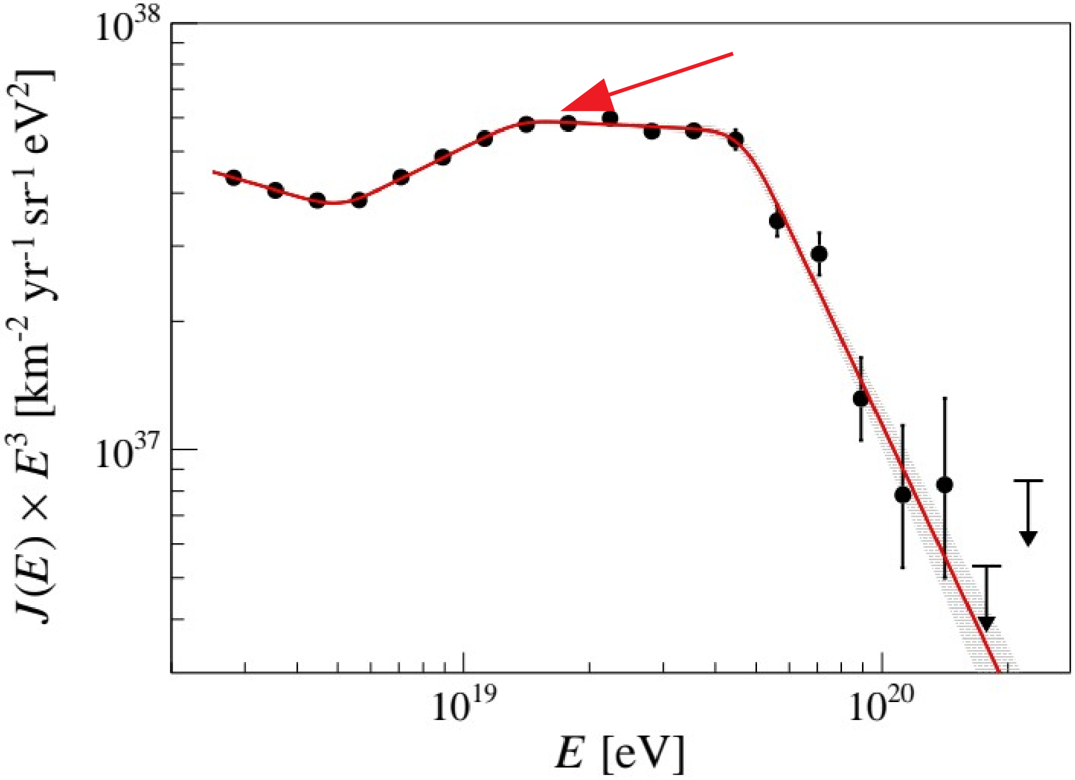

$$J(E) = J_0 \left(\frac{E}{10^{18.5}\ \text{eV}}\right)^{-\gamma_1} \prod_{i=1}^{3} \left[1 + \left(\frac{E}{E_{ij}}\right)^{1/\omega_{ij}}\right]^{(\gamma_i-\gamma_j)\omega_{ij}}$$

Ankle and suppression are confirmed

New feature at 1.3×10^19 eV detected (3.9 σ)

Consistency with other experiments

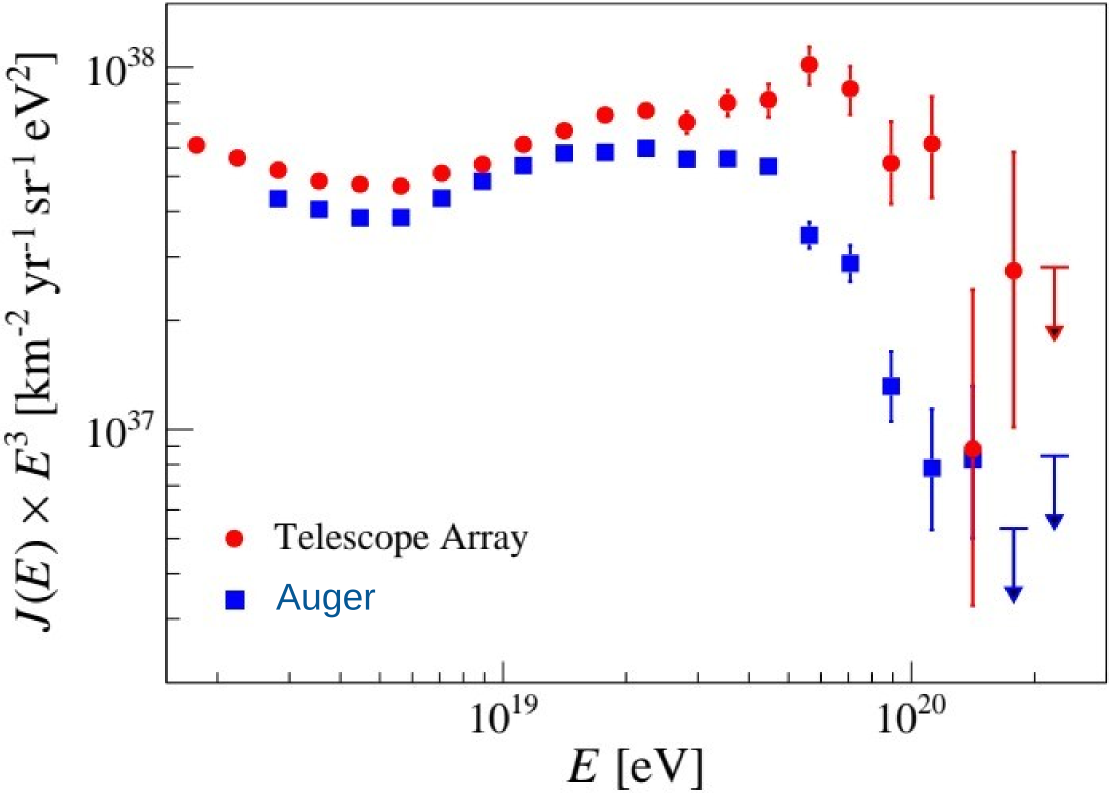

Telescope Array: hybrid CR observatory on the northern hemisphere (Utah)

Spectra consistent within systematics until 10^{19} eV (ΔE_{Auger}=±14%; E_{TA}=21%)

10% mismatch per energy decade above 10^{19} eV

Origin of mismatch under investigation
- Energy dependent systematics?
- North south asymmetry in the sky?

Spectra in common declination band shows some inconsistency at $E>10^{19}$ eV

Common Auger and TA Working Group investigating such differences

Dependence on declination

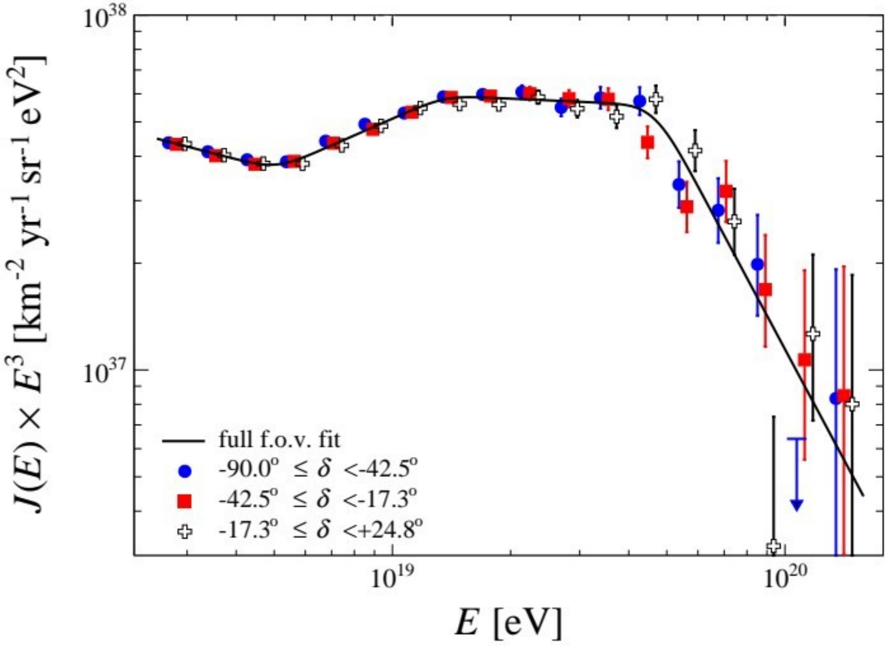

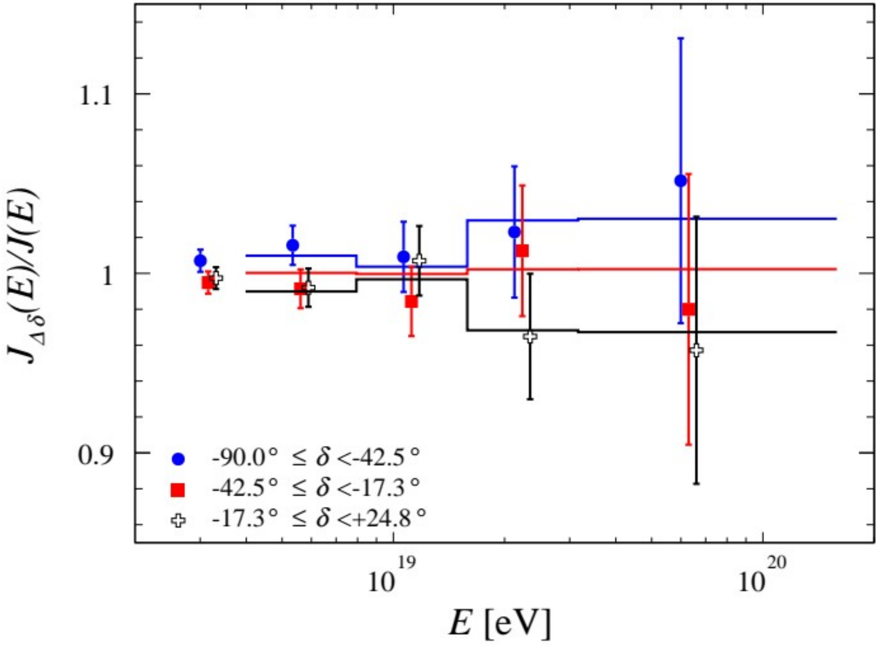

No dependence of the spectrum on the declination

Mild excess from the south due to the measured dipole anisotropy

Difference with TA possibly due to systematics?

Interpretation of the results

Reconstruct the UHECR source properties

Fit of a simple astrophysical model to the spectrum and composition data above $10^{18.7}$ eV

Input:

- Homogeneous and isotropic source distribution
- Few representative masses injected
- Injected spectrum: PL with exponential cutoff
- Propagation effects modeled
- EAS modeled (hardonic interaction models)

Output:

- Expected spectrum
- Expected composition
- Expected photon flux
- Expected neutrino flux

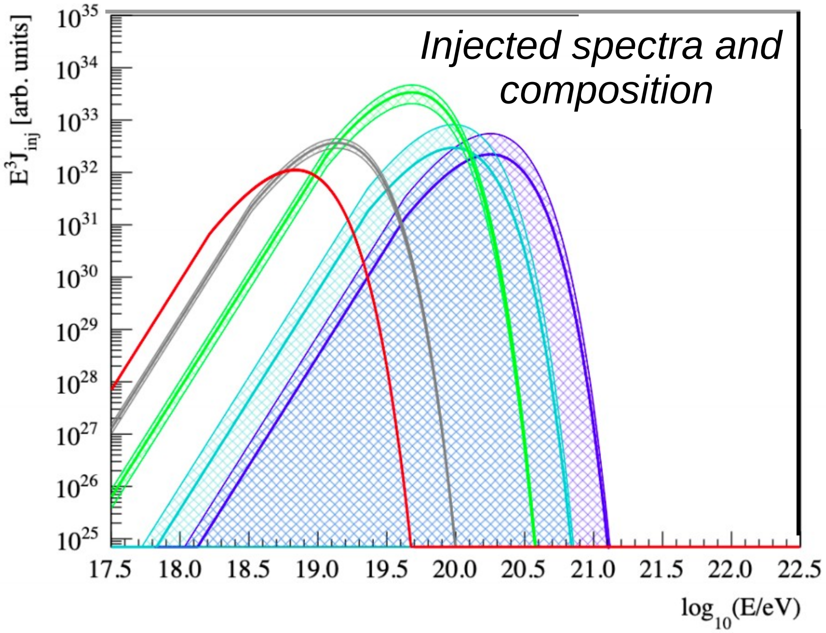

Background photons model

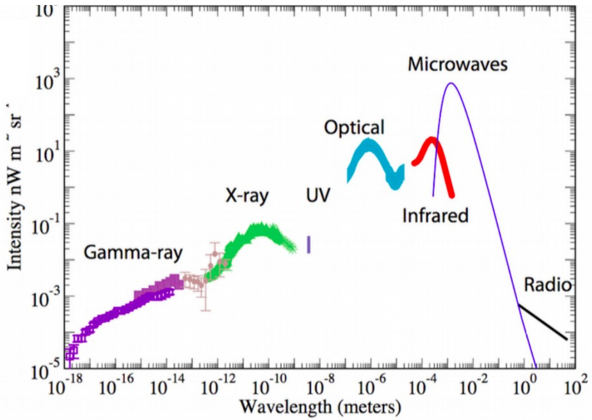

Interpretation of the results

Spectrum and composition data are consistent with a **rigidity dependent scenario**

New feature @10^{19} eV: interplay between helium to CNO component

Suppression: acceleration maximum + propagation effects

Steepening and suppression rigidity dependent features?

- $E_{34} / E_{23} = 3.4$
- $Z_N / Z_{He} = 3.5$

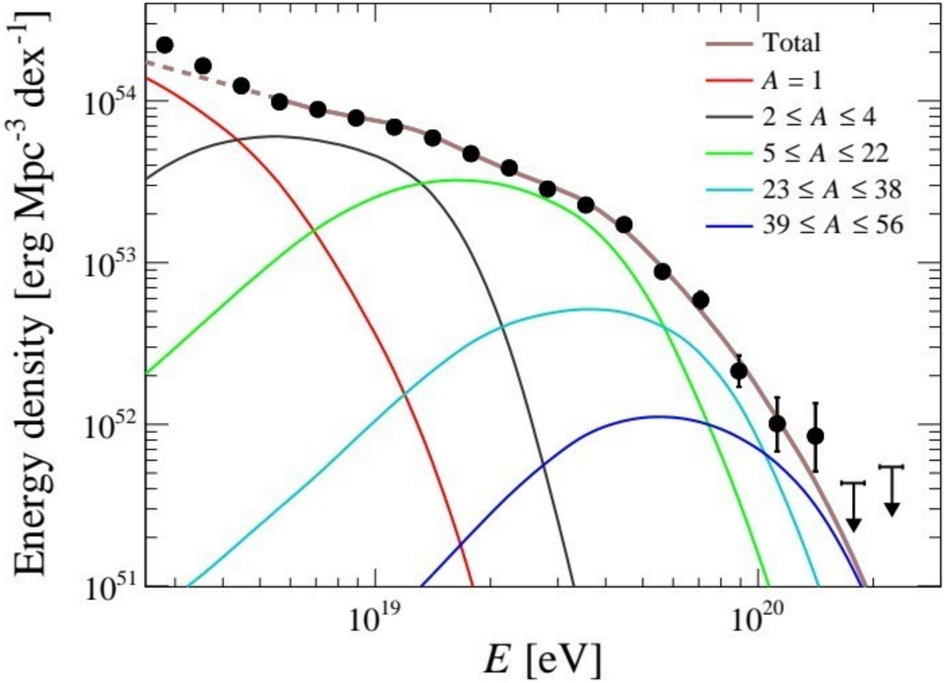

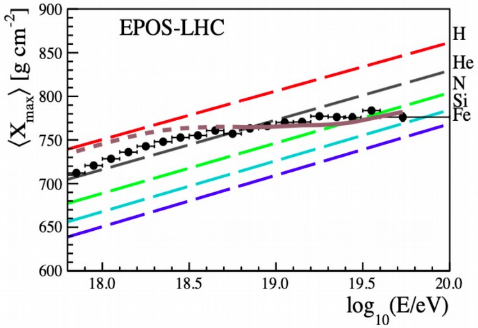

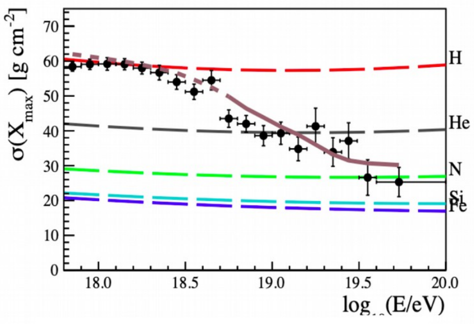

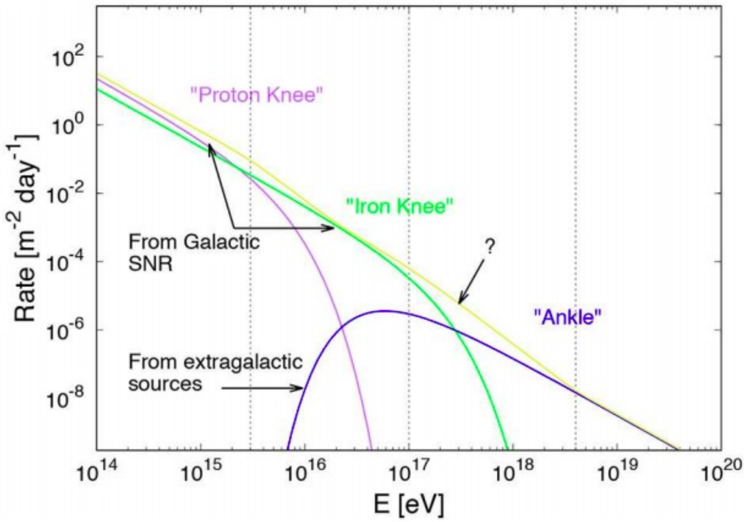

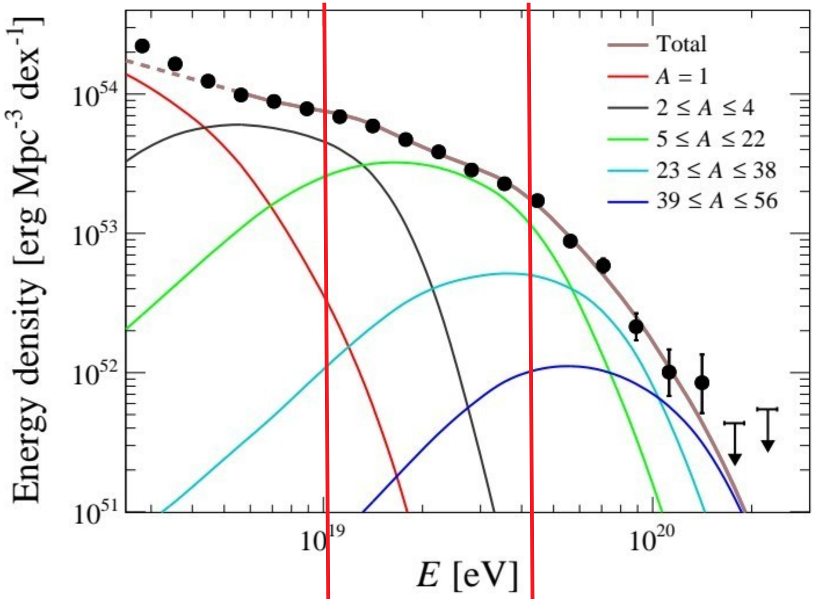

Composition in the 10^{17}- $10^{18.5}$ range still under study

Combined fit being extended under the ankle

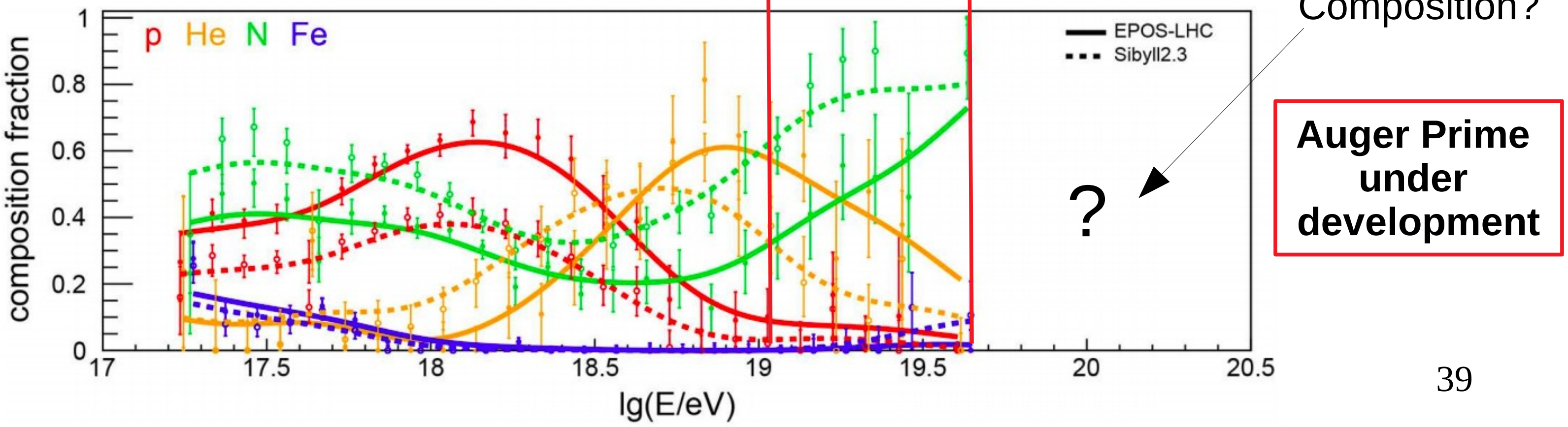

Auger Prime under development

Alves Batista et al.,
Front. Astr. Sp. Sci. (2019)

Conclusions

The Pierre Auger Observatory revolutionized the understanding of CR at the most extreme energies (suppression confirmed, anisotropy studies, mass composition at the highest energies, stringent limits on neutral particles...)

The measurement of the spectrum:

- **Combination of different techniques over 4 orders of magnitude**
- **Most precise measurement of the vertical spectrum until above $10^{18.4}$ eV**
- **Main spectral features confirmed**
- **New feature detected at 1.3×10^{19} eV**
- **Astrophysical interpretation consistent with rigidity dependent scenario**

Backup slides

Auger Prime

SurfaceScintillator Detector (SSD)
(Mass composition measurement)

Upgraded detector electronics
(Improve the performances of the WCD)

Small PMT
(Increase the dynamic range of the WCD)

Radio antenna
(Measure the radio emission of showers)

Underground Muon Detector
(Direct muon measurement)

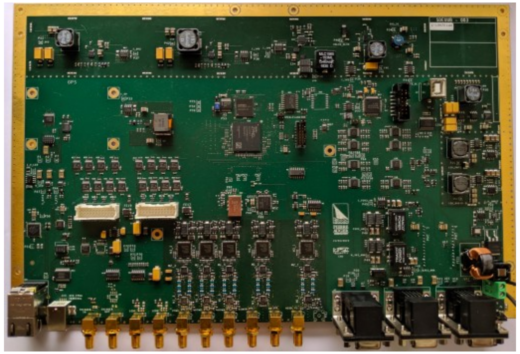

Auger Prime (nature of Suppression)

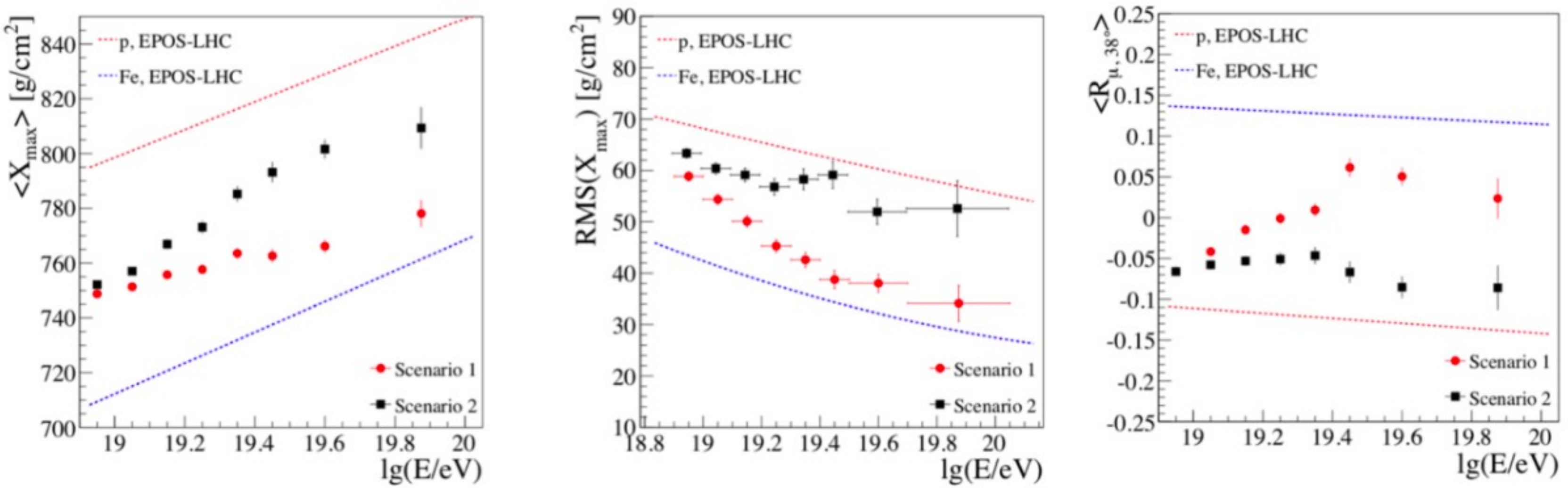

Maximum rigidity
Propagation

What is the nature of the suppression?

- Maximum rigidity effect
- Propagation (photodisintegration) effect

Addition of a scintillator on top of WCD to increase composition sensitivity until 10^{20} eV

A. Castellina EPJ web of Conferences 210 06002 (2019)

The energy calibration of the SD

Energy scale of SD detector based on golden hybrid events
(Events with FD and SD reconstruction)

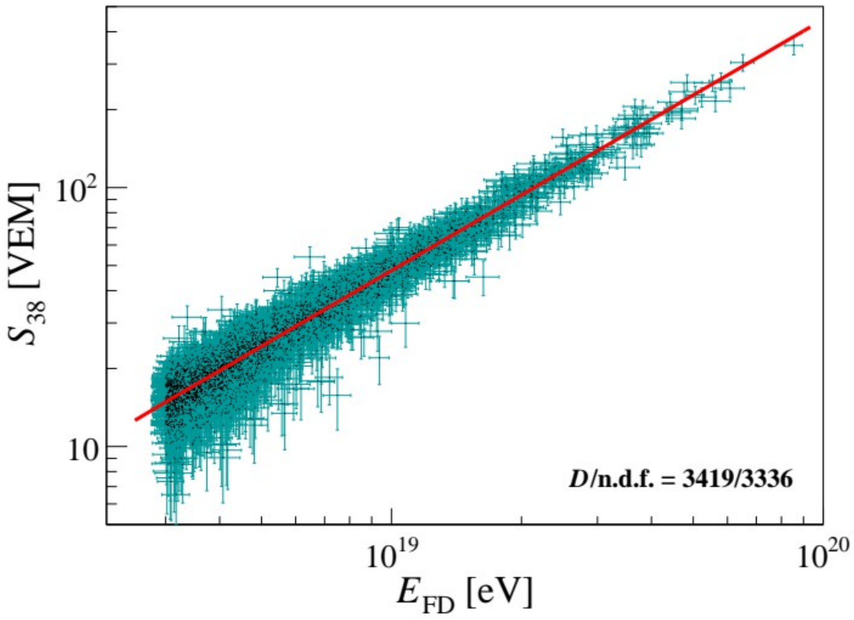

Relation between E_{FD} and shower size (S) is fit with

$$E_{FD} = A\,S^B$$

Unbinned maximum likelihood method

$$\ln \mathcal{L} = \sum_k \ln f(E_{\mathrm{FD}k}, S_{\mathrm{SD}k}) = \sum_k \ln \left(\frac{1}{N} \sum_i G(E_{\mathrm{FD}k} | E_{\mathrm{FD}i}, \sigma_{\mathrm{FD}i}) G(S_{\mathrm{SD}k} | S(E_{\mathrm{FD}i}), \sigma_{\mathrm{SD}i}) \right)$$

PDF for detection of an event with size S_{SD} and E_{FD}

FD resolution function

SD resolution function

The Surface Detector exposure

The detectors are deployed on an hexagonal grid

Fiducial cut: accept only 6T5 events

6T5 events: station with highest signal surrounded by 6 active stations

Aperture of each of such cells $A_{cell} = 4.59\ km^2\ sr\ yr$

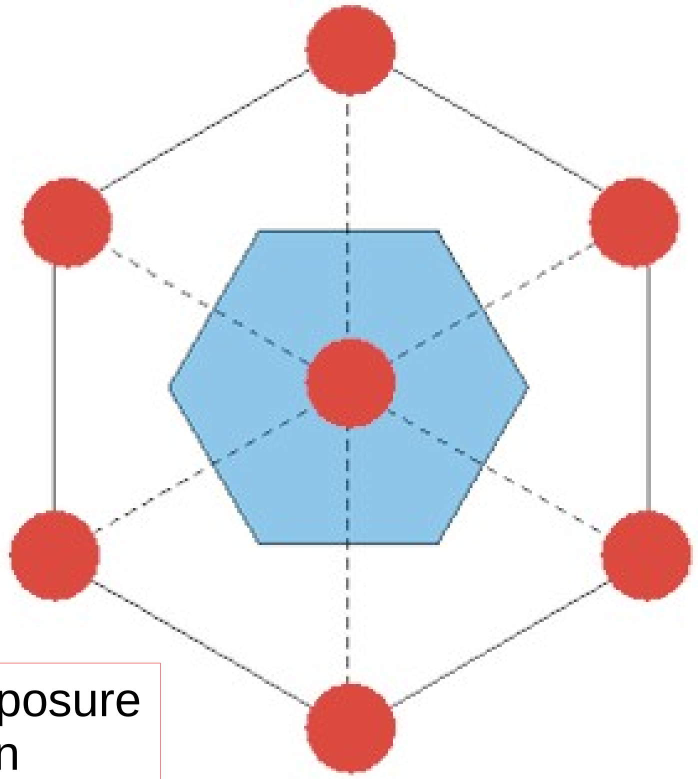

$$\mathcal{E} = \int_{\Delta t} N_{cell}(t)\, A_{cell} \cos(\theta)\, dt\, d\Omega$$

Geometrical exposure calculation above threshold
No MC